

MOCCA-III: Effects of pristine gas accretion and cluster migration on globular cluster evolution, global parameters and multiple stellar populations

M. Giersz¹, A. Askar¹, A. Hypki^{1,2}, J. Hong⁴, G. Wiktorowicz¹, L. Hellström¹

¹ Nicolaus Copernicus Astronomical Center, Polish Academy of Sciences, ul. Bartycka 18, PL-00-716 Warsaw, Poland
e-mail: mig@camk.edu.pl

² Faculty of Mathematics and Computer Science, A. Mickiewicz University, Uniwersytetu Poznańskiego 4, 61-614 Poznań, Poland

³ Korea Astronomy and Space Science Institute, Daejeon 34055, Republic of Korea

Accepted XXX. Received YYY; in original form ZZZ

ABSTRACT

Using the *moCCA* code, we study the evolution of globular clusters with multiple stellar populations. For this purpose, the *moCCA* code has been significantly extended to take into account the formation of an enriched population of stars from re-accreted gas with a time delay after the formation of the pristine population of stars. The possibility of cluster migration in the host galaxy and the fact that the pristine population can be described by a model, not in virial equilibrium are also taken into account. Gas re-accretion and cluster migration have a decisive impact on the observational parameters of clusters and the ratio of the number of objects between the pristine and enriched populations. The obtained results, together with observational data, suggest a speculative scenario that makes it possible to explain observational data, the correlation between the mass of the cluster and the ratio of the pristine to the enriched populations, and the observational fact that for some globular clusters, the pristine population is more concentrated than the enriched one. In this scenario, it is important to take into account the environment in which the cluster lives, the conditions in the galaxy when it formed, and the fact that a significant part of the globular clusters associated with the Galaxy come from dwarf galaxies that merged with the Milky Way. The initial conditions describing GCs in the simulations discussed in the paper are different from typical initial GC models that are widely used. Instead of GCs being highly concentrated and lying deep inside the Roche lobe, models that fill the Roche lobe are required. This carries strong constraints on where in the galaxy GCs are formed.

Key words. stellar dynamics – methods: numerical – globular clusters: evolution – stars: multiple stellar populations

1. Introduction

Historically, globular clusters (GCs) have for many decades been thought of as gravitationally bound large collections of stars that formed over a short period of time and have a uniform chemical composition. Observations, both spectroscopic and photometric, made in recent decades have forced a revision of this view. GCs have been shown to contain different stellar populations that differ significantly in chemical composition, especially in light element content. A thorough description of the observational data and their analysis leading to the explanation of the phenomenon of multiple stellar populations (MSPs) can be found in excellent review papers, (e.g. Gratton et al. 2019; Bastian & Lardo 2018; Milone & Marino 2022).

Observations, both spectroscopic and photometric, provide the following information:

1. Star-to-star light element abundance variations: He, C, O, N, Na, Mg, Al. Abundances are correlated (Na-N and N/Na-He) or anti-correlated (Na-O and N-C). This points out for hot hydrogen burning through CNO-, NeNa-, and MgAl-cycles (e.g. Langer et al. 1993). Such correlations and anti-correlations are present for the whole range of CMD diagrams, from the bottom of MS up to RGB and HB, and also for WD cooling sequence (Dondoglio et al. 2021);
2. There is very small Fe spreads allowed of about ~ 0.1 dex (e.g. Marino et al. 2019). There are some exceptions e.g. NGC 6341 (Lee 2023);
3. There is practically no time spread between populations. It should be at most a few hundred Myr (e.g. Nardiello et al. 2015; Lucertini et al. 2021);
4. Enriched population (POP2) is centrally concentrated, but there are some exceptions (e.g. Leitinger et al. 2023). One of the possible origins of the reversed spatial distribution is a merger of clusters (e.g. Lee 2015);
5. MSP are very obvious in massive (larger than $\sim 10^4 M_{\odot}$) and old clusters and are observed not only in MW but also in nearby dwarf galaxies. It seems that massive young clusters, younger than ~ 2 Gyr, do not contain MSPs (e.g. Niederhofer et al. 2017; Martocchia et al. 2017). The observational ratio between number of stars from POP2 to the total number of stars in the cluster (N_2/N_{tot}) is between 0.3–0.4 and 0.9;
6. Fraction of enriched stars increases with cluster mass, may also increase with cluster age (e.g. Milone et al. 2020);
7. MSPs are also related to differences in kinematic properties and binary content between populations. POP2 stars have more radially anisotropic velocity distributions (e.g. Li-bralato et al. 2019, 2023), a more rapid rotation (e.g. Kamann et al. 2020a; Cordoni et al. 2020; Szigeti et al. 2021), a lower fraction of binaries (e.g. Lucatello et al. 2015; Kamann et al. 2020b; Milone et al. 2020)

The above observational findings impose strong constraints on models explaining the formation of MSPs in GCs. The observed correlations and anti-correlations between light elements suggest the need for dilution of the ejected products of thermonuclear reactions from stars/binary systems with remnants of the gas after pristine population (POP1) formation. The observed large N_2/N_{tot} ratios suggest a very efficient and rapid process of POP1 star loss from the cluster. It is estimated that POP1's mass loss should be about 90% of its initial mass (e.g. Bastian & Lardo 2018). The observed correlation between the current GC mass and the N_2/N_{tot} ratio imposes the strongest constraints on the models and probably suggests a strong influence on the environment in which GCs form and live.

Several scenarios have been proposed that attempt to explain the emergence and continued evolution of MSP. These models can be divided into two groups. The first group, in which the formation of POP2 is shifted in time relative to POP1 and requires the re-accretion of gas on GC and its mixing with matter ejected by AGB stars, belongs to the AGB scenario (e.g. D'Antona et al. 2002; D'Ercole et al. 2008; D'Antona et al. 2016; Calura et al. 2019). The second group belongs to models in which POP2 is formed at virtually the same time as POP1 and does not require the re-accretion of gas by the GC. Matter ejected from massive stars and binary systems mixes with residual primordial gas. These scenarios include: interacting massive binaries (de Mink et al. 2009), fast-rotating massive stars (Prantzos & Charbonnel 2006; Decressin et al. 2007), the early disc accretion (Bastian et al. 2013), very massive stars (Vink 2018; Higgins et al. 2023), very massive stars due to runaway collisions (Denissenkov & Hartwick 2014; Gieles et al. 2018), nucleosynthesis in accretion disks around stellar-mass black holes (Breen 2018; Fréour et al. 2024) and recently renewed single-binary composite scenario (Vanbeveren et al. 2012; Bekki 2023). It has also been proposed that POP1 stars moving through a medium polluted by AGB and massive star ejecta could form and subsequently accrete enriched substellar companions (Winter & Clarke 2023). Some of these scenarios will be discussed in detail later in Section 4. Unfortunately, as pointed out in the excellent review paper by Bastian & Lardo (2018), no scenario can explain a significant number of observational facts.

In recent years, there have been many attempts and simulations with various numerical codes to obtain a model corresponding to the MSP observations. Monte Carlo (e.g. Vesperini et al. 2021; Sollima 2021; Hypki et al. 2022, 2024), NBODY (e.g. Lacchin et al. 2024), hydrodynamic (e.g. Calura et al. 2019; McKenzie & Bekki 2021; Yaghoobi et al. 2022) and semi-analytical (e.g. Bekki 2023; Parmentier 2024) codes have been used for this purpose. Despite the success in reproducing some observational properties of GCs from MSP, these simulations were associated with important simplifying assumptions about the effect of gas re-accretion on GCs, the time of formation and parameters describing POP2, as well as the effect of external conditions on the evolution of GCs. Because of the above, it is important to check whether the results obtained so far concerning mass, half-mass radius (R_h) of GCs, or N_2/N_{tot} ratio will be maintained when a more physical prescription of POP2 formation is introduced and the influence of the external environment is taken into account, at least partially and in a simplified manner.

To test how the inclusion of environmental effects and the effect of mass re-accretion on GCs and the time shift of POP2 formation affects the evolution of stellar populations in GCs and whether the constraints and results obtained from previous simulations are still correct, the *moCCA* code was substantially up-

dated. The expansion of the *moCCA* code will allow us to follow in a simplified way the evolution of GCs with MSPs in a variable galactic environment the influence of the parameters describing the formation of POP1 and POP2 and the parameters defining their spatial and kinematic characteristics. We expect that these extensions will allow a better understanding of the evolution of GCs with MSPs, bring closer to a more accurate reproduction of the observations, and impose stronger constraints on the initial conditions and physical processes responsible for the formation of MSPs in GCs.

The paper is organized as follows. Section 2 describes the latest version of the *moCCA* code with all added extensions and the initial conditions of the numerical simulations performed for this paper. Section 3 presents the results obtained with the *moCCA* simulations through the ratio N_2/N_{tot} , R_h , and cluster mass. In Section 4 we discuss the potential implications obtained from *moCCA* simulations for the observational signatures of the multiple populations in GCs and some implications for the scenarios of their formation. We also provide a speculative scenario explaining the observational parameters of Milky Way GCs (MWGCs) and the correlation between cluster mass and N_2/N_{tot} ratio. Section 5 briefly summarizes the main findings of the paper and describes future works.

2. Method

This section presents the description of the *moCCA* code with all additions needed to follow the evolution of GCs with re-accreted gas. All parameters needed to describe the MSP and GCs are also discussed here.

2.1. *MOCCA* code

This work is based on the numerical simulations performed with the *moCCA* Monte Carlo code (Giersz 1998; Hypki & Giersz 2013; Giersz et al. 2013; Hypki et al. 2022, 2024). *moCCA* is an advanced code that performs full stellar and dynamical evolution of real size star clusters up to Hubble time. *moCCA* can follow the full dynamical and stellar evolution of MSPs. For mergers and mass transfers between stars from different populations we only assume that they form a so-called mixed population because we do not provide procedures to accurately model the chemical mixing between two stars belonging to different populations. Strong dynamical interactions in *moCCA* are performed with *FEWBODY* code (Fregeau et al. 2004; Fregeau & Rasio 2007). The dissipative effects connected with tidal forces or gravitational wave radiation during dynamic interactions are not taken into account in the simulations performed for this paper.

The implementation of stellar and binary evolution within the *moCCA* code is based on the rapid population synthesis code *BSE* code (Hurley et al. 2000, 2002) that has been strongly updated by Belloni et al. (2017, 2018), Banerjee et al. (2020), and Kamlah et al. (2022). The stellar/binary evolution parameters used in the presented simulations are referred to as Model C in Kamlah et al. (2022). In short, the metallicity of both populations in all the simulated models was set to $Z = 0.001$. The updated treatment for the evolution of massive stars was used according to Tanikawa et al. (2020) together with improved treatment for mass loss due to stellar winds and the inclusion of pair and pulsational pair-instability supernova (Belczynski et al. 2016). The masses of black holes (BH) and neutron stars (NS) were determined according to the rapid supernovae prescriptions from Fryer et al. (2012). NS natal kicks were sampled from a Maxwellian distribution with $\sigma = 265$ km/s (Hobbs et al. 2005).

However, for BHs, these natal kicks were reduced according to the mass fallback prescription (Belczynski et al. 2002; Fryer et al. 2012). The formation of neutron stars with negligible natal kicks through electron-capture or accretion-induced supernova was also enabled. Another feature of these models is the inclusion of gravitational wave (GW) recoil kicks whenever two BHs merge (Baker et al. 2008; Morawski et al. 2018)). It was assumed low birth spins for BHs with uniformly sampled values between 0 and 0.1 (Fuller & Ma 2019). The orientation of the BH spin relative to the binary orbit is randomly distributed (Morawski et al. 2018).

2.1.1. MSP in the MOCCA code

In two previous papers (Hypki et al. 2022, 2024), the evolution of GCs with MSPs under the asymptotic giant branch (AGB) scenario (e.g. D’Ercole et al. 2008, 2010, 2012; Conroy & Spergel 2011; D’Antona et al. 2016; Calura et al. 2019) was studied using the *moCCA* code (Hypki & Giersz 2013; Giersz et al. 2013; Kamlah et al. 2022). In those simulations, it was assumed for simplicity, that the process of formation of distinct populations of stars in a GCs occurs simultaneously. At the start of the simulations, the two stellar populations are already formed and are together in virial equilibrium (hereinafter, the model will be referred to as no time delay MSP - nTD-MSP). Simulations have shown that models of clusters that are close to the Milky Way (MW) center, in which the POP1 fills the Roche lobe and the POP2 is strongly concentrated toward the center reproduce very well the ranges of the ratio N_2/N_{tot} and the ranges of global observational parameters of MWGCs, such as the cluster mass and its R_h . Despite these successes, the nTD-MSP model implemented in the *moCCA* code had very serious drawbacks, namely: it did not take into account the fact that the formation of POP2 is delayed in time relative to the time of POP1 formation and the re-accretion of gas surrounding the just-formed cluster, which then mixes with enriched material from the ejected envelopes of AGB stars. To address these problems, the *moCCA* code has been expanded with the inclusion of the following features:

- Time delay for forming POP2 stars relative to POP1 stars;
- Time delay in re-accretion of the gas surrounding the cluster;
- Consideration of the mass of ejected AGB star envelopes in the formation process of POP2 stars,
- Migration of globular clusters (GCs) to larger Galactocentric distances.

The new model will be referred to as time-delay MSP (TD-MSP).

In addition, the process of cluster migration due to dynamical friction has also been implemented in the *moCCA* code, based on the work of Arca-Sedda & Capuzzo-Dolcetta (2014). In this paper, simulation results from cluster evolution with dynamical friction included are not discussed. Dynamical friction affects cluster evolution only for galactocentric distances less than 2 kpc, so it is not significant for the evolution of the clusters discussed in this article.

Implementing the new functionality in the *MOCCA* code required quite deep changes related to the fact that POP2 objects are treated as gas rather than stars for a certain time (POP2 formation delay time – t_{delay}). In the following subsections, we will describe, step by step, the changes made to the *moCCA* code

2.1.2. POP2, gas re-accretion and star formation

To reflect the complex process of gas re-accretion onto a GC, we made the following simplifying assumptions. The parameters of POP1 are determined by: the initial model (usually King (1966) model), the ratio of the tidal radius (R_t) to the half-mass radius (R_{h1}), the initial mass function (IMF), including the maximum stellar mass ($m_{1\text{max}}$) and the virial ratio (Q_1), which can be different than 0.5. POP2 is drawn in a similar manner to POP1 with one exception. POP2’s concentration is controlled by a parameter conc_{pop} equal to the ratio of POP2’s half-mass radius to POP1’s half-mass radius ($\text{conc}_{\text{pop}} = R_{h2}/R_{h1}$). Both populations are not forced to be together in virial equilibrium as in the case of the nTD-MSP model. POP2 until time t_{delay} does not change its spatial distribution, the position of each star/binary system, treated as a gas particle, does not change over time, it is constant. Only POP1 objects undergo both dynamical and stellar evolution. POP2 objects, up to the time t_{delay} , contribute only as a source of gravitational potential and do not participate in any interactions with POP1 objects.

In the *moCCA* code, the simulation of the complex pristine gas re-accretion process is controlled by four parameters, namely: the initial time at which gas re-accretion starts (t_{start}), the time of completion of the accretion process (t_{end}), which is usually equal to the t_{delay} , the mass of the pristine gas that remained in the cluster after POP1 formation (M_{start}), the total mass of accreted gas (M_{end}). In addition to the mass of accreted gas, the mass of ejected matter from AGB stars is added on an ongoing basis. From a technical point of view, all POP2 objects up to t_{delay} time are treated as variable mass gas particles. The mass of the gas particles varies linearly in time from t_{start} to t_{end} , from M_{start} to M_{end} , which mimics the gas re-accretion process. After time t_{delay} , all gas particles are instantly converted into stars and binary systems according to the previously drawn population of stars/binary systems and their parameters. The conversion of gas particles into stars occurs at the beginning of the next time step. From then on, POP2 objects take part in stellar evolution, relaxation, and all types of dynamic interactions. In a future version of the *MOCCA* code, the conversion of gas particles into stars will be staggered in time and will depend on the mass of the star. More massive stars will be converted earlier.

2.1.3. Cluster migration

Many previous works indicate that the process of GC formation occurs in the early stages of galaxy formation when the environment is highly variable and strongly influences the movement of clusters in the galaxy and their evolution (e.g. Kruijssen 2015; Forbes et al. 2018; El-Badry et al. 2018; Meng & Gnedin 2022; De Lucia et al. 2024). Meng & Gnedin (2022) used cosmological simulations for MW-type galaxies to study the effects of the galaxy’s strong and rapidly varying tidal field on the motion of clusters and the probability of their survival. They showed that GCs that formed very close to the galactic center (less than 1-2 kpc) over a period of about 1 Gyr increase their orbit by a factor of at least two. In the current version of the *moCCA* code, the orbit of a cluster can only be circular, and the mass of the galaxy within that orbit is concentrated at the center (point mass). Thus, the implementation of the migration of GCs’ orbits in the *moCCA* code is made only for circular orbits whose size changes by a factor of $\text{frac}_{\text{tidal}}$. This change is performed stepwise at the beginning of a new time step when the cluster lifetime exceeds the t_{tidal} critical value. In the new version of the code, the change in orbit size will be spread over time, and the fact that GCs’ orbits

are eccentric will be taken into account. For this purpose, the idea proposed by Cai et al. (2016) will be used to compare the mass loss averaged over the cluster orbit for eccentric and circular orbits. They showed that for an eccentric orbit, it is possible to assign a circular orbit for which GC will have on average the same mass loss as in an eccentric orbit. This is a very rough solution but will enable the `MOCCA` code to be used for the first time to study the evolution of clusters with eccentric orbits and in the variable tidal field of the galaxy.

2.2. Initial conditions

Initial conditions for `MOCCA` simulations studying the evolution of GCs with MSPs can be divided into two groups, namely: those related to the global parameters of the cluster and the environment in which it moves, and to the technical parameters describing the stellar populations. Global parameters are: the number of objects in the cluster (N_1 – remember that at the beginning only POP1 is present and it constitutes the entire cluster), the size of the GC circular orbit relative to the galactic center (R_g), King parameter describing the initial model (W_{01}), the virial ratio for POP1 (Q_1), the factors describing the migration of the cluster ($\text{frac}_{\text{tidal}}$ and t_{tidal}), whether or not the cluster initially fills the Roche lobe (TF or nTF), the half-mass radius of the cluster (R_h , remember that at the beginning it is equal to R_{h1}), the initial mass function (IMF), the upper mass limit for POP1 ($m_{1\text{max}}$), the binary fraction along with the parameter distributions of binary systems. The technical parameters are the number of POP2 stars (N_2), the King parameter describing the model (W_{02}), the concentration parameter conc_{pop} , the virial coefficients for POP2 (Q_2), the upper mass limit for POP2 stars ($m_{2\text{max}}$), and the parameters describing the re-accretion of gas: t_{start} , t_{end} , t_{delay} , M_{start} , M_{end} . The ranges of the above parameters are summarized in Table 1. The table requires a few comments to facilitate its analysis. It is important to emphasize that in the TD-MSP model, initially, the GC consists only of POP1 stars. Thus, all initial global cluster parameters refer only to POP1. Once the evolution of POP2 is started at time t_{delay} , which in simulated models is always equal to t_{end} , the cluster's global parameters refer to both populations, POP1 and POP2. Please keep this fact in mind when analyzing the figures in Section 3. The number of parameters that determine the models with MSP is very large, and it would not be practical to run simulations with all combinations of these parameters. Only simulations with a representative subset of the parameters have been calculated, so that meaningful conclusions can be drawn about the dependence of observational GC parameters on their combinations. We computed about 100 `MOCCA` models for this paper.

3. Results

In this section, we will analyze the impact of gas re-accretion, cluster migration, and each of the individual global and technical parameters, described in the previous section, on the evolution of the cluster mass, R_h , and ratio N_2/N_{tot} .

3.1. Gas re-accretion and migration

Before we begin to study the effect of global and technical parameters on the evolution of observable cluster parameters (henceforth when we talk about global observational parameters of GCs we mean the following parameters: cluster mass, R_h , and ratio N_2/N_{tot}), we would like to focus first on the effect

that gas re-accretion and cluster migration bring to the observable parameters. All simulations to date of the evolution of GCs with MSP performed under the AGB framework have assumed for simplicity that: POP2 is formed and evolves together with POP1 (Vesperini et al. 2021; Hong et al. 2019; Hypki et al. 2022, 2024), that POP2 is formed with AGB ejecta and pristine gas left after POP1 formation (Sollima 2021) and that POP2 is formed from re-accreted gas with a fixed POP1 potential (Calura et al. 2019). Those simulations did not take into account the effects on the properties of POP1 connected with the slow accumulation of re-accreted gas in the cluster center.

The evolution of the cluster with the gas re-accretion and cluster migration are depicted in Figure 1 and Figure 2, respectively. Assuming that the GC is in quasi-dynamical equilibrium, we can, using the virial theorem, determine how the R_h will evolve when the cluster loses mass or gains it. When it loses mass the characteristic radius (R_h) should increase, and when it gains mass it should decrease. In Figure 1 left panel we see exactly this behavior. First, as the cluster loses mass due to stellar evolution and tidal stripping the R_h increases (black solid and dashed lines). As the re-accretion of gas begins, the R_h strongly decreases from 50 Myr to 100 Myr (solid black line). The decreasing R_h for the nTD-MSP model is associated with tidal stripping. It continues until the end of evolution and is related to the fact that the cluster is TF. For the TD-MSP model, re-accretion of gas causes the R_h to decrease and cluster to become nTF. The next increase in R_h is related to the fact that the cluster is free to expand until it again becomes TF. The evolution of the cluster mass behaves as expected. For the nTD-MSP model, it decreases continuously due to stellar evolution and tidal stripping. For the TD-MSP model, it first decreases due to stellar evolution and tidal stripping, then increases strongly when POP2 objects are included, and then decreases as in the nTD-MSP model. We know from the previous studies (e.g. Hypki et al. 2022, 2024) that the ratio N_2/N_{tot} strongly depends on whether the cluster is TF or how strongly nTF it is. The more nTF the cluster is, the less this ratio increases due to fewer escaping stars. So the effect of gas re-accretion should lead to much smaller observed values of this ratio. Indeed, we can observe this type of evolution in the right panel of Figure 1. The ratio N_2/N_{tot} for the model without gas re-accretion is significantly larger than for the model with gas re-accretion. This difference can be as high as 0.3.

The migration of GCs to greater galactocentric distances will be associated with an increase in the cluster's R_t . Assuming a point mass of the galaxy and a flat rotation curve, the R_t is a function of galactocentric distance and cluster mass, $R_t \sim R_g^{2/3} (M/M_\odot)^{1/3}$. Increasing R_t will cause the cluster to no longer be TF and become nTF. The consequence will be a significant slowdown in the growth or freezing of the ratio N_2/N_{tot} . Since the cluster is no longer limited by R_t it can expand freely. This will lead to an increase in R_h and slow the cluster's mass loss. Indeed, these predictions are confirmed in Figure 2. In the left panel, we can see a significant increase in R_h and a slowdown in mass loss when the galactocentric distance is increased. In the right panel, the ratio N_2/N_{tot} is practically constant after increasing the galactocentric distance. In conclusion, the migration of clusters to larger galactocentric distances will result in GCs having larger masses and R_h and a significantly smaller N_2/N_{tot} ratio. This is not a combination that would help explain the observed parameters of GCs. In the following Sections, we will try to find combinations of global and technical MSP parameters that will bring the cluster models closer to the observed parameters for MWGCs

Table 1. Global and technical parameters for simulations with MSP. The meaning of the parameters is as follows: N_1 and N_2 – number of POP1 and POP2 objects respectively; W_{o1} and W_{o2} – King model parameters for POP1 and POP2 respectively; Q_1 and Q_2 – virial parameters; R_g – the size of the GC circular orbit; R_{h1} – half-mass radius of POP1; tidal field – tidally filling (TF) or underfilling (nTF); IMF – initial mass function; binary fraction – the ratio between the number of binaries and total objects; t_{tidal} – time when GC orbit size increases; conc_{pop} – the ratio of half-mass radii (R_{h2}/R_{h1}); $m_{1\text{max}}$ and $m_{2\text{max}}$ – maximum stellar masses; t_{start} – initial time of gas re-accretion; t_{end} – completion time of accretion; M_{start} and M_{end} – mass of pristine and accreted gas respectively.

Global Parameters									
N_1	R_g	Q_1	W_{o1}	$\text{frac}_{\text{tidal}}$	t_{tidal} (Gyr)	Tidal Field	R_{h1}	IMF	Binary Fraction
400,000	1	0.5	3	1	1000	TF	1	Kroupa (2001), $m_{1\text{max}} = 150M_{\odot}$	95%
800,000	2	0.6	4	2	1	nTF	2		
1,600,000	4	0.7	5						
3,200,000			6						
Technical Parameters									
N_2	N_2/N_{tot}	W_{o2}	conc_{pop}	Q_2	$m_{2\text{max}}(M_{\odot})$	t_{start} (Myr)	t_{end} (Myr)	$M_{\text{start}}(M_{\odot})$	$M_{\text{end}}(M_{\odot})$
50,000	150,000 / 550,000	7	0.05	0.5	20	$0.05 \times t_{\text{end}}$	50	0	Mass computed from N_2 , IMF and ejected by AGB stars
100,000	50,000 / 850,000		0.1		8	$0.5 \times t_{\text{end}}$	100		
150,000	100,000 / 900,000		0.2				equal to t_{delay}		
200,000	300,000 / 1,200,000								
300,000	400,000 / 2,000,000								
400,000	200,000 / 3,400,000								

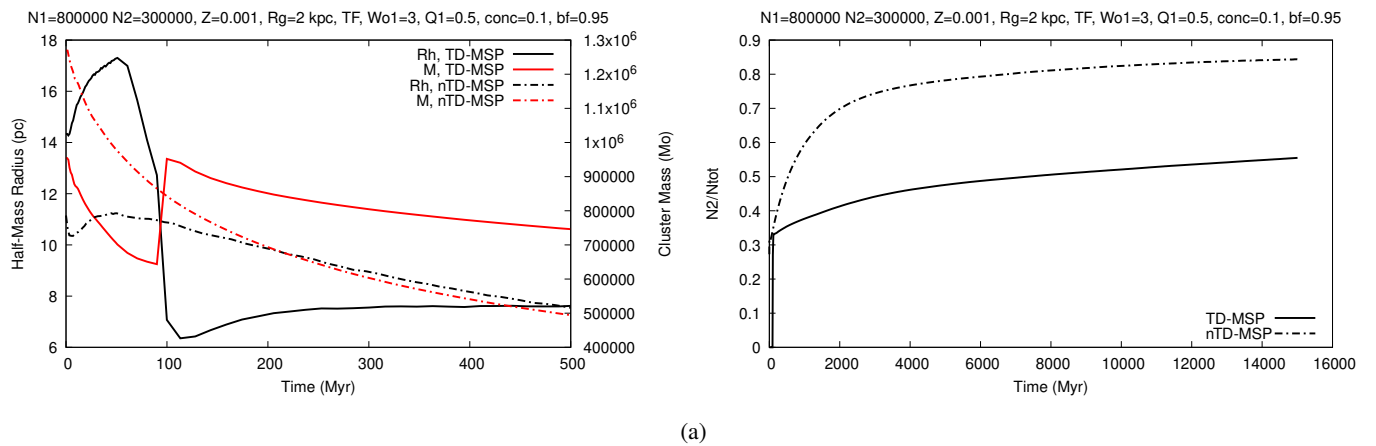
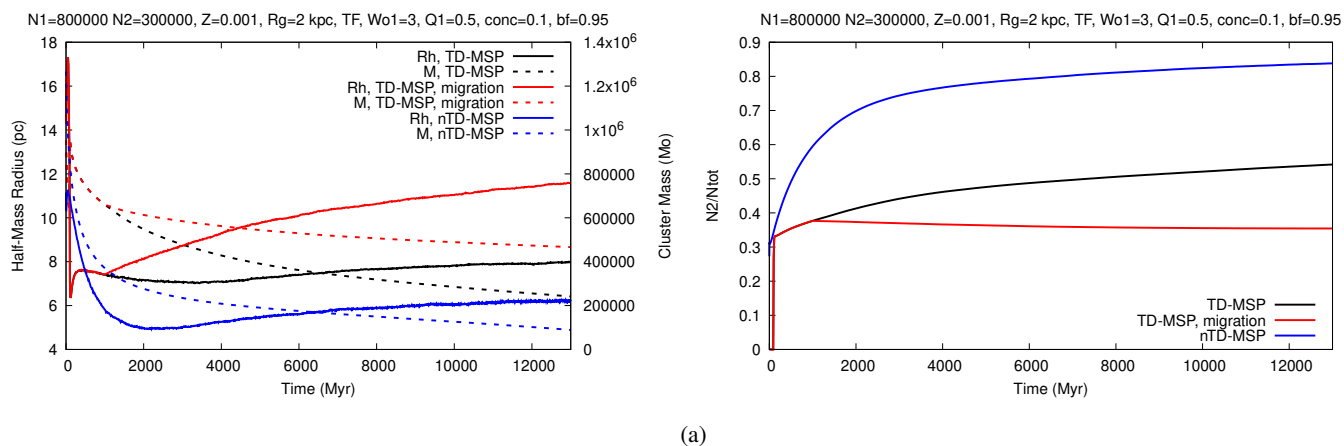


Fig. 1. Left panel: evolution of R_h for nTD-MSP model (red solid line), and TD-MSP model (black solid line) and evolution of the total cluster mass for nTD-MSP model (red dashed dot line), and TD-MSP model (black dash-dotted line). Right panel: evolution of the ratio N_2/N_{tot} for the nTD-MSP model (black dash-dotted line), and TD-MSP model (black solid line). The global cluster parameters are listed at the top of each panel: N_1 - number of POP1 objects, N_2 - number of POP2 objects, Z - metallicity, R_g - galactocentric distance (size of the circular orbit), TF - tidally filling POP1, W_{o1} - King parameter for POP1, conc - concentration parameter ($\text{conc}_{\text{pop}} = R_{h2}/R_{h1}$), bf - binary fraction, Q_1 - virial ratio for POP1. Unless otherwise noted, all Figures from now on are made for the parameters: $t_{\text{start}} = 0.5 * t_{\text{delay}}$ and $t_{\text{end}} = t_{\text{delay}} = 100$ Myr.

3.2. Number of POP1 and POP2 objects

When studying the effect of the number of POP1 objects on the observational properties of clusters, we must also consider the number of POP2 objects. Figure 3 shows models with the different N_2/N_{tot} ratios for different numbers of POP1 objects. Generally speaking, more massive clusters have a longer half-mass relaxation time, a larger R_t for the same galactocentric distance, and a larger R_h . Thus, the evolution of GCs with more POP1 and POP2 objects will be slower and clusters will be able to survive longer than clusters with fewer objects. Since the time scale of the evolution of clusters with fewer objects is faster, we can expect the N_2/N_{tot} ratio to grow faster than for clusters with more objects. The larger the number of objects, the slower the N_2/N_{tot} ratio grows. Indeed, the described evolution of cluster observational parameters is fully reflected in Figure 3. An interesting effect can be observed in the left panel of Figure 3 for the evolution of R_h . The smaller the initial mass of the cluster, the faster the dissolution of the cluster. The fast cluster dissolution occurs due to the presence of the black hole subsystem (BHS). The dis-

solution process is described in detail in the work of Giersz et al. (2019). Just before dissolution, the structure of the cluster is very characteristic. The cluster has a mass of about a few thousand M_{\odot} and R_h of a few pc, i.e. it is very bloated. The right panel of Figure 3 shows the evolution of the N_2/N_{tot} ratio. The smaller the number of POP2 objects with the same number of POP1 objects, the higher the final value of the N_2/N_{tot} ratio. This is due to the fact that in the models presented in the paper, the King parameter for POP1 is $W_{o1} = 3$. This means that the cluster was initially only slightly concentrated to the center and very sensitive to tidal stripping. The small mass of POP2 objects implies only a slight reduction in R_h due to gas reaccretion. That is when POP2 is switched on, the cluster is still not highly concentrated and will lose mainly POP1 objects due to tidal stripping. Note an interesting feature visible in this figure, namely, for small initial values of N_2/N_{tot} the increase of N_2/N_{tot} occurs slowly, then accelerates after about 1 Gyr of evolution to grow at the end of the cluster evolution to values characteristic of MWGCs. The small N_2/N_{tot} values for young clusters may be a response to observational data suggesting that young and massive star clus-



(a)

Fig. 2. Left panel: evolution of R_h for nTD-MSP model (blue solid line), TD-MSP model (black solid line) and TD-MSP model with migration (red solid line) and evolution of the total cluster mass for nTD-MSP model (blue dashed line), TD-MSP model (black dashed line) and TD-MSP model with migration (red dashed line). Right panel: evolution of the ratio N_2/N_{tot} for nTD-MSP model (blue solid line), TD-MSP model (black solid line), and TD-MSP with migration model (red solid line). The global cluster parameters are listed at the top of each panel and are the same as for Figure 1. Note the small reduction in the value of the N_2/N_{tot} ratio for the model with migration. It is related to the fact that after migration POP1 objects do not escape at the same rate as before, and to the fact that mainly POP2 objects are ejected from the cluster as a result of dynamic interactions.

ters (YMSC) do not exhibit POP2 objects. This problem will be discussed in detail in Section 4.

3.3. King Parameter W_{01}

The works of [Vesperini et al. \(2021\)](#); [Hypki et al. \(2022\)](#) have clearly shown that for the AGB scenario of MSP formation, associated with gas re-accretion and ejected AGB envelopes, POP1 must initially be TF and have a small concentration toward the center for the N_2/N_{tot} ratio to be comparable to the values observed in MWGCs. This condition for initial models described by the King parameter means that W_{01} should be less than 6 or 5. Generally speaking, we expect that the smaller the W_{01} , the smaller the cluster mass, the larger the R_h after the gas re-accretion, and the larger the N_2/N_{tot} ratio. The further evolution is controlled by the escape speed. The larger the W_{01} , the higher the escape velocity and the smaller the stream of escaping objects from the cluster. Accordingly, the rapid loss of cluster mass and the associated decline in R_t should lead to a rapid decline in R_h and its relative stabilization when the BHS is responsible for the evolution of the cluster. Indeed, this type of behavior of global cluster parameters with increasing W_{01} can be observed in Figure 4. There seems to be no monotonic dependence on W_{01} for R_h evolution. It seems that for $W_{01} = 5$ there is a trend reversal, for larger W_{01} , the level of almost constant R_h (associated with balanced BHS evolution) decreases instead of increasing. This is connected with a larger escape speed for larger W_{01} models. In addition, it seems that for $W_{01} = 4$ the system does not show the characteristics of balanced evolution - R_h is continuously decreasing. This is an unexpected effect that requires further investigation. It seems that despite the presence of the BHS, the period of evolution in which cluster expansion associated with the energy generated by binary systems balances tidal stripping may not always be clearly marked.

3.4. POP2 concentration parameter

The concentration parameter (conc_{pop}) is defined as the ratio of the half-mass radius of POP2 to the half-mass radius of POP1.

Thus, a cluster with a smaller conc_{pop} should be more concentrated have a higher escape velocity and become more nTF after POP2 formation. This means that the larger the conc_{pop} , the larger the mass of the cluster, the larger the R_h , and the smaller the N_2/N_{tot} ratio. Indeed, in Figure 5 we observe exactly such an evolution of GC global parameters depending on conc_{pop} . It is noteworthy that the differences between the evolution of the cluster with different conc_{pop} do not result in a large change in the cluster's global parameters.

3.5. Galactocentric distance

The R_t , assuming a constant rotational velocity of the galaxy and a circular orbit of the cluster, is just a function of the mass of the cluster and the R_g . This means that, for the same cluster mass, the greater the R_g , the greater the R_t . Since the cluster is TF this means that, for the same cluster spatial structure, the larger the R_t the larger the R_h and the half-mass relaxation time, and thus slower is the dynamical evolution of the cluster. In summary, the larger the R_g the larger the mass of the cluster, the larger R_h , and the smaller the N_2/N_{tot} ratio. Indeed, we can observe this type of evolution of global cluster parameters in Figure 6. The cluster with the smallest R_g is characterized by the smallest R_h , mass and evolution time, and the largest N_2/N_{tot} ratio. It is important to draw attention to the fact that dependence on R_g is important from the point of view of MWGC observational parameters. In the TD-MSP model, it is very difficult to obtain a range of MWGCs observational parameters, such as relatively small R_h or very large cluster masses. The solution, at least partially to this problem, is the formation of GCs very close to the center of the galaxy. This problem will be discussed in depth in Section 4.

3.6. POP1 virial ratio

The important parameter describing MSP in the TD-MSP model is the virial ratio Q_1 for POP1. The process of star cluster formation is still a hot topic, not yet fully solved. However, it seems that the fact of strong expansion of the cluster after residual gas removal after the formation of the first stellar population

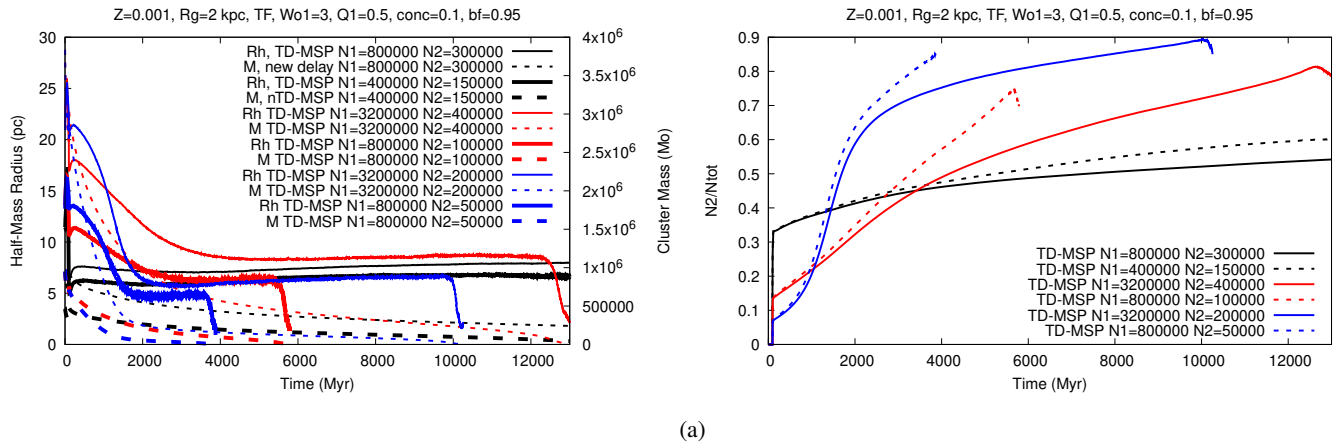


Fig. 3. Left panel: evolution of R_h (solid lines) and the cluster total mass (dashed lines) for TD-MSP models with different numbers of POP1 objects and POP2 objects. Right panel: evolution of the ratio N_2/N_{tot} for TD-MSP models with different numbers of POP1 objects and POP2 objects. The global cluster parameters are listed at the top of each panel and are the same as for Figure 1.

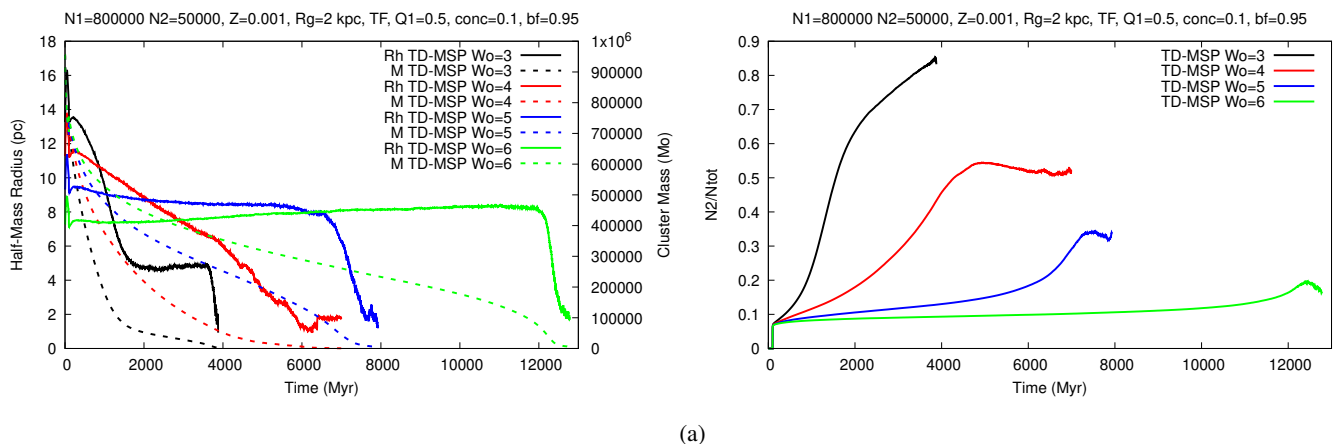
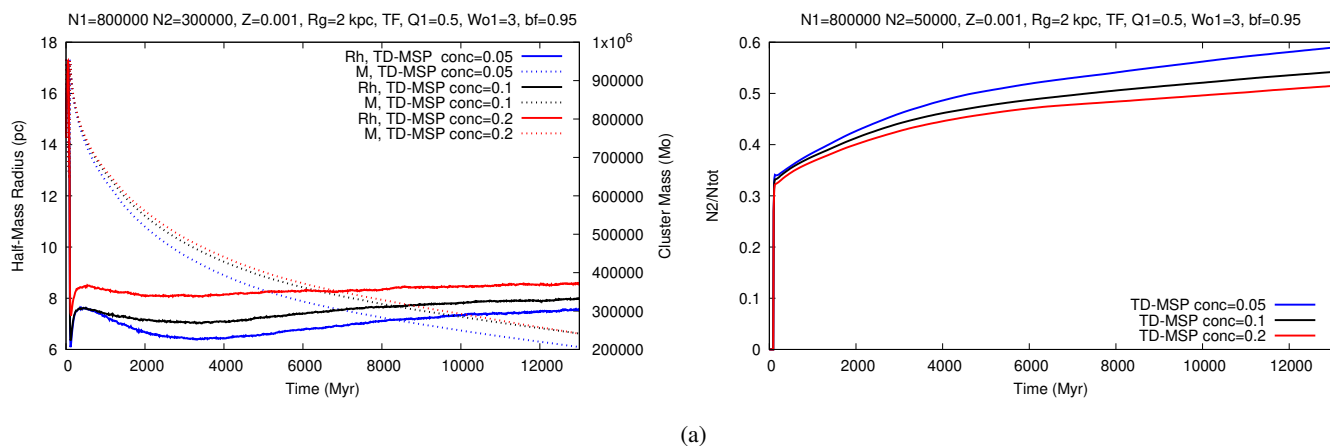


Fig. 4. Left panel: evolution of R_h (solid lines) and the cluster total mass (dashed lines) for TD-MSP models with different King parameter W_{o1} . Right panel: evolution of the ratio N_2/N_{tot} for TD-MSP models with different King parameter W_{o1} . The global cluster parameters are listed at the top of each panel and are the same as for Figure 1.

is strongly established. Therefore, the assumption that initially POP1 is outside virial equilibrium and has $Q_1 > 0.5$ is fully natural. Overall, for systems with $Q_1 > 0.5$, we should expect stronger mass loss and tidal stripping, which will lead to lower cluster mass, lower R_h , and a higher N_2/N_{tot} ratio. A model with a larger Q_1 is characterized by an excess of kinetic energy relative to potential energy. Therefore, the spatial distribution of stars is less concentrated and stars can escape from the system more easily. This leads to a sharp loss of POP1 stars and a sharp decrease in R_h and a strong increase in the N_2/N_{tot} ratio. Indeed, this type of evolution is observed in Figure 7. The dependence of the evolution of the cluster's global parameters on Q_1 seems crucial to reconstruct the range of global parameters observed in MWGCs. By taking into account the dependence on Q_1 , we can obtain R_h of several pc, and N_2/N_{tot} ratio greater than 0.8, but we cannot reproduce the observational relationship between cluster mass and N_2/N_{tot} - the greater the mass of the cluster, the greater the N_2/N_{tot} ratio. This problem and its possible solution will be discussed in Section 4.

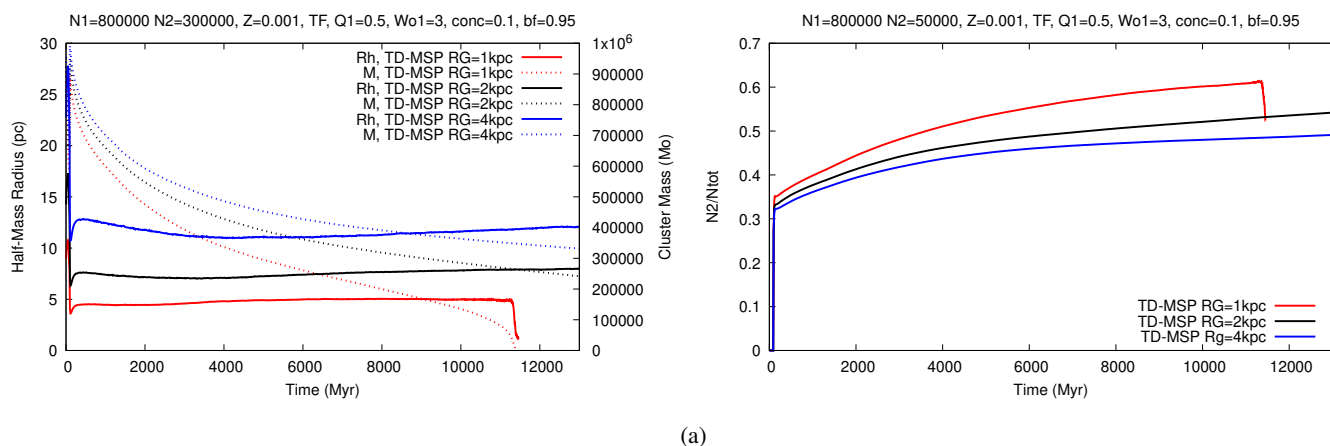
3.7. Maximum IMF mass for POP2

The maximum mass of stars formed in POP2 is a quantity that is very difficult to determine within the framework of theory as well as observations. Therefore it is usually assumed, for simplicity, that POP2 is formed with the same IMF as POP1, only the maximum mass of main sequence stars is much smaller for POP2 than for POP1. This limitation is related to the fact that for POP2 no significant differences in metal content are observed between POP1 and POP2 objects. This means that in POP2 supernovae (SNe) outbursts should be kept to a minimum in order not to contaminate with metals the gas from which the less massive POP2 stars are formed. By reducing the maximum mass for IMF from $20 M_{\odot}$ to $8 M_{\odot}$, we should expect a smaller reduction in R_h as a result of gas re-accretion and a smaller cluster mass and a lower N_2/N_{tot} ratio. This is because a cluster with a smaller IMF maximum mass is less massive than a cluster with a larger IMF maximum mass (with the same IMF). Thus, a cluster with a larger maximum IMF mass has a larger R_i and thus R_h . Larger R_h also means a little more mass loss by the cluster and consequently larger N_2/N_{tot} . Indeed, we can observe such behavior in Figure 8, which shows the evolution of the cluster mass, R_h , and the N_2/N_{tot} ratio as a function of the maximum IMF mass.



(a)

Fig. 5. Left panel: evolution of R_h (solid lines) and the cluster total mass (dashed lines) for TD-MSP models with different POP2 concentration parameters ($\text{conc} = \text{conc}_{\text{pop}}$). Right panel: evolution of the ratio N_2/N_{tot} for TD-MSP models different $\text{conc} = \text{conc}_{\text{pop}}$. The global cluster parameters are listed at the top of each panel and are the same as for Figure 1.



(a)

Fig. 6. Left panel: evolution of R_h (solid lines) and the cluster total mass (dashed lines) for TD-MSP models with different galactocentric distance (R_g). Right panel: evolution of the ratio N_2/N_{tot} for TD-MSP models different R_g . The global cluster parameters are listed at the top of each panel and are the same as for Figure 1.

Changing the maximum IMF mass has only a small effect on the evolution of these parameters. Of course, the number of BHs or NSs will change and will be slightly smaller (about 5%) for a maximum IMF mass of $8 M_{\odot}$. Such small changes do not have a strong influence on the GC evolution.

The above results suggest that the maximum IMF mass does not have a key effect on the global observational parameters of GCs, provided that it is not too large and affects the metallicity of POP2, or too small to allow the survival of GCs that are TF and have a non-concentrated POP1 with small W_{o1} .

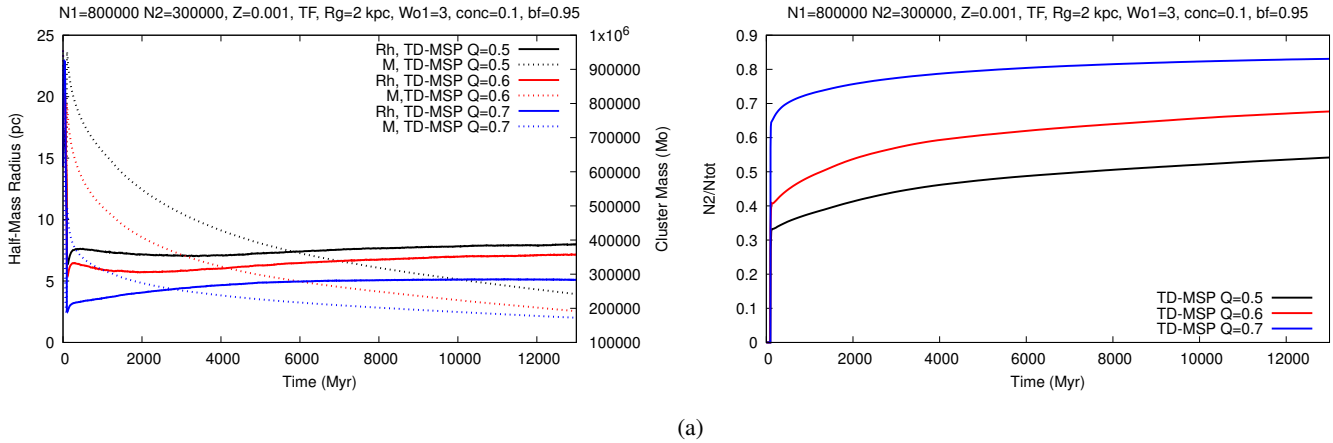
3.8. Time of gas re-accretion

The implementation of the AGB scenario for MSP formation in the `MOCCA` code is based on several technical parameters, in particular, those describing the time of the start of gas re-accretion (t_{start}) and the time of POP2 formation (t_{delay} - see Table 1). These parameters affect the scale of cluster expansion associated with mass loss due to stellar evolution and the scale of R_h decrease. The earlier the start of gas re-accretion, the smaller the initial R_h expansion and the smaller the mass loss of the cluster. Similarly, the later the time of POP2 formation, the greater the expansion of R_h and the greater the cluster's mass loss. Since the mass of

re-accreted gas is independent of the technical parameters, we can expect that the magnitude of the reduction in R_h and the increase in cluster mass after POP2 formation will be similar to the values obtained in the reference model. We can only expect minor differences related to an earlier or later start of the evolution of POP2 objects, and a slightly reduced rate of mass loss by POP1. Thus, the observational parameters of GCs discussed in the paper should not show a significant dependence on the technical parameters describing gas re-accretion. Indeed, these predictions are confirmed by the simulations shown in Figure 9. The long-scale evolution of GCs should not significantly depend on the time of the start of gas re-accretion and the time of POP2 formation. Other model parameters related to the structure of POP1 and POP2 and the environment in which the cluster moves are of key importance and provide an opportunity to estimate these parameters by comparing models with observations.

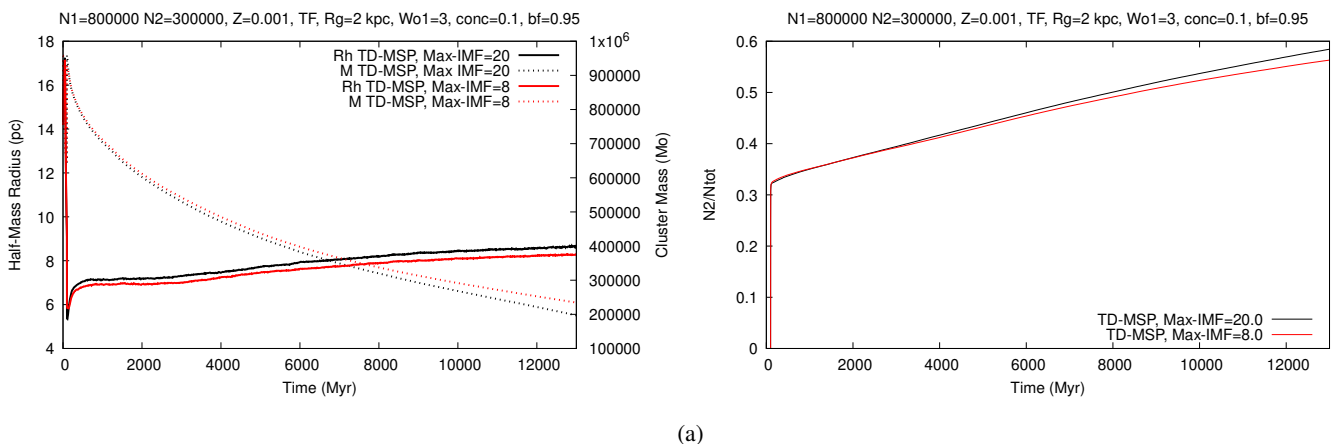
3.9. Brief summary

In two previous papers (Hypki et al. 2022, 2024), it was shown that under the scenario nTD-MSP the evolution of globular clusters with MSP can successfully reproduce the observational parameter ranges of MWGCs. However, a very serious flaw in this



(a)

Fig. 7. Left panel: evolution of R_h (solid lines) and the cluster total mass (dashed lines) for TD-MSP models with different Q_1 . Right panel: evolution of the ratio N_2/N_{tot} for TD-MSP models different Q_1 . The global cluster parameters are listed at the top of each panel and are the same as for Figure 1.



(a)

Fig. 8. Left panel: evolution of R_h (solid lines) and the cluster total mass (dashed lines) for TD-MSP models with different maximum IMF mass for POP2 objects, Right panel: evolution of the ratio N_2/N_{tot} for TD-MSP models different maximum IMF mass for POP2 objects. The global cluster parameters are listed at the top of each panel and are the same as for Figure 1.

model was the assumption that both populations arise simultaneously and both are in virial equilibrium. To break free from this assumption, the TD-MSP model was introduced, in which the formation of POP2 arises at a certain time after POP1. In addition, GCs can migrate to greater galactocentric distances after a certain evolutionary time. The new models are characterized by many parameters described in Table 1. Unfortunately, the introduction of the TD-MSP model has resulted in global model parameters that less closely reproduce the observational parameters of MWGCs; in particular, the N_2/N_{tot} ratio is clearly smaller, R_h rises to much higher values and cluster mass is smaller than that of nTD-MSP. This is very evident for models with migration.

Of course, by manipulating the global and technical parameters describing MSPs, one can try to get model parameters more in line with MWGCs, i.e. R_h within a few pc, N_2/N_{tot} within 0.3 to 0.9, and masses up to several hundred thousand M_{\odot} . The most promising factors are:

- Number of POP2 objects (N_2): A smaller N_2 leads to a higher N_2/N_{tot} ratio and a smaller half-mass radius (R_h). Unfortunately, the final mass of the GC is too small.
- Number of POP1 objects: A larger number of POP1 objects slows cluster evolution. When combined with a small num-

ber of POP2 objects, this can support cluster survival until Hubble time.

- Central concentration of POP1 (W_{01}): A smaller W_{01} results in a smaller R_h and cluster mass, a higher N_2/N_{tot} ratio, but also leads to significantly faster cluster evolution.
- Galactocentric distance (R_g): A smaller R_g leads to a smaller R_h and cluster mass, a higher N_2/N_{tot} ratio, but also results in faster cluster evolution.
- Virial parameter (Q_1): A larger Q_1 results in a smaller R_h and cluster mass, a higher N_2/N_{tot} ratio, but also leads to significantly faster cluster evolution.

It seems that Q_1 is the most promising parameter to obtain the observational values of N_2/N_{tot} and R_h in the TD-MSP models. Unfortunately, the combination of this parameter with other parameters will not allow to obtain cluster masses in their upper observable values. The solution may be another mechanism related to the environment in which GCs live. In the next Section, we will discuss possible solutions to this problem.

4. Discussions

This Section will focus on briefly summarizing the observational material collected mainly photometrically (MOCCA simulations

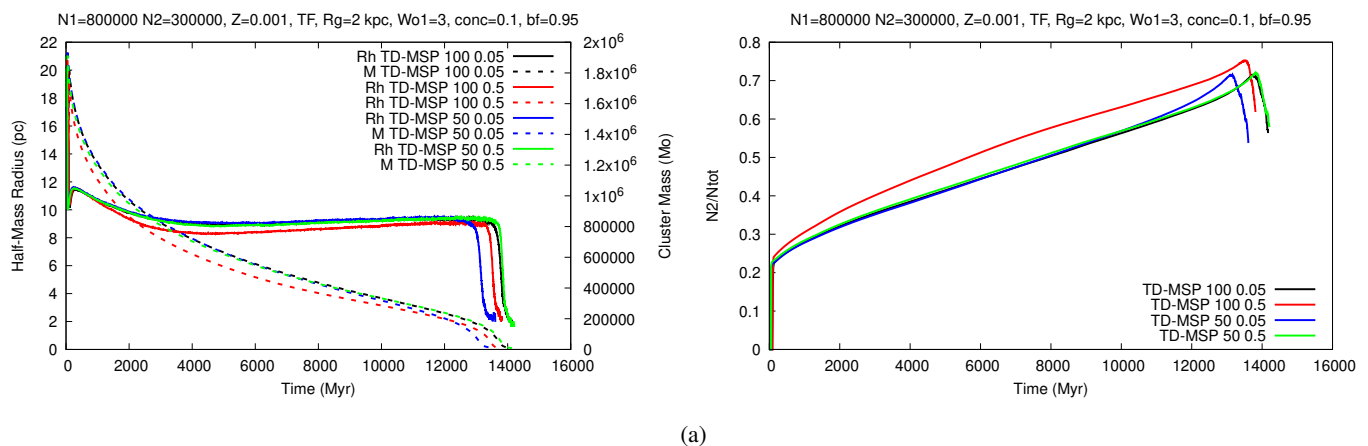


Fig. 9. Left panel: evolution of R_h (solid lines) and the cluster total mass (dashed lines) for TD-MSP models with different time of gas re-accretion (combination of $t_{delay} = t_{end}$ time (100 or 50 Myr) and the fraction of t_{delay} time at which the gas re-accretion starts (t_{start} : 0,05 or 0.5)) Right panel: evolution of the ratio N_2/N_{tot} for TD-MSP models different time of gas re-accretion. The global cluster parameters are listed at the top of each panel and are the same as for Figure 1.

only with this type of observations can be compared) for GCs with MSP. We will then provide a brief description of the scenarios proposed to explain MSP, discuss the weaknesses, and identify the question marks associated with these scenarios. We will then present a speculative scenario, based on the AGB model and *moCCA* simulations, for the emergence and evolution of MSP.

4.1. Observations

The observational characteristics of GCs with MSP are very extensively and critically discussed in the excellent review paper by Bastian & Lardo (2018). Briefly, the following facts about MSP in GCs have solid observational confirmation.

1. Massive GCs are composed of stars exhibiting differences in light element content. Correlations and anti-correlations between the contents of these elements indicate that they must have been formed by thermonuclear reactions of hydrogen burning at very high temperatures, which can happen only in the case of massive stars;
2. MSPs are characterized by a very small range of Fe abundances (only about 0.1 dex);
3. Differences in the ages of different populations are very small, only of the order of a few tens of Myrs;
4. POP2 is centrally concentrated relative to POP1 (Mastrobuono-Battisti & Perets 2021), however, see the recent work of Leitinger et al. (2023);
5. MSPs are observed in different galactic environments. Clusters with too low masses or too young do not seem to show MSP. The critical mass seems to be around $10^5 M_\odot$ and age smaller than 1 – 2 Gyr (Milone et al. 2020; Leitinger et al. 2023);
6. There is a relatively strong correlation between GC mass and N_2/N_{tot} ratio;
7. N_2/N_{tot} ratio does not seem to correlate clearly with other global parameters of GCs.

Any scenario attempting to explain the formation of MSPs in GCs must take into account the above observational facts. An additional complication is the fact of the violent process of MW formation associated with multiple close interactions and mergers with nearby dwarf galaxies. In the course of this many GCs

associated with dwarf galaxies have been intercepted and accreted by the MW (e.g. Chen & Gnedin 2024). The population of MWGCs is a collection of GCs formed in different environments, and this fact must be taken into account when we try to understand the observational facts of MSP and compare them with simulations of the evolution of GCs.

The *moCCA* code can be used to study the evolution of GCs located only in circular orbits around the galactic center, assuming the galaxy’s point mass, the mass that is contained within the cluster’s orbit. This assumption is at odds with the orbits of MWGCs (e.g. Bajkova & Bobylev 2021). In order to be able to compare the results of simulations with observations, we used the work of Cai et al. (2016) in which the authors define a circular orbit, which is characterized by a similar cluster mass loss as the cluster being in an eccentric orbit. The relationship between circular orbit and eccentric orbit parameters is as follows, $R_c = a(1 + e)(1 - 0.71e)^{(5/3)}$, where R_c is the radius of the circular orbit, and a and e are the semi-major axis and eccentricity, respectively. Of course, the formula based on Table 1 in Cai et al. (2016) is very approximate, but nevertheless, it gives some insight into the rate of evolution of the MWGC, which can be compared with that obtained in *moCCA* simulations. Note that mass loss of GCs is the main factor responsible for the evolution of the N_2/N_{tot} ratio. Thus, a reasonably accurate way to establish the relationship between the actual and simulated evolution of GCs in numerical models is crucial to better understand the observations of MWGCs. Recently, Chen & Gnedin (2024) published a paper in which they analyzed 10 structural and kinematic observational parameters of MWGCs to determine which GCs formed in-situ and which ex-situ. They estimated that about 60% of the MWGCs were formed in-situ. Using their results, we will present figures defining the relationship of the observational parameters with the type of their formation.

The observational data shown in Figures 10–12 are from the following MWGC catalogs: Milone et al. (2017) for N_2/N_{tot} ratios, Bajkova & Bobylev (2021) for kinematic parameters, Chen & Gnedin (2024) for origin types, and Baumgardt et al. (2019) for global parameters. Figure 10 shows N_2/N_{tot} ratios as a function of cluster mass (left panel) and radius of the circular orbit (right panel). In the left panel we can clearly see, widely discussed in the literature, the correlation between N_2/N_{tot} and cluster mass. The correlation is relatively strong and, interest-

ingly, shows no significant differences between clusters formed in-situ and ex-situ. It seems that this type of correlation could indicate the effect of the tidal field of the parent galaxy. Tidal field forces are similar, which means that GCs in dwarf galaxies should form closer to the center than in MW. The right panel reveals an interesting (maybe expected) dependence on the radius of the circular orbit. Ex-situ GCs have average orbit radii significantly larger than in-situ clusters. In general, most in-situ clusters have radii of circular orbits contained within 7 kpc (see also Figures 11 and 12).

Figure 11 shows cluster metallicity as a function of cluster mass (left panel) and the radius of the circular orbit (right panel). In the right panel, we can see that in general there is no obvious relationship between cluster mass and metallicity, except for the fact that ex-situ clusters show a smaller spread of metallicity, and a large fraction of in-situ clusters have higher metallicity than ex-situ clusters. In the right panel, we see a very clear dependence on the radius of the circular orbit. Ex-situ clusters have, on average, a lower metallicity than in-situ clusters and are distributed over much more wide orbits than in-situ clusters. This is even more pronounced than in Figure 10.

Figure 12 shows the mass of the cluster as a function of the radius of the circular orbit (left panel) and the eccentricity of the cluster's orbit as a function of pericenter distance (right panel). As we expected after analyzing the previous figures, there is no dependence of the cluster mass on the radius of the circular orbit. Ex-situ GCs have a similar mass distribution to in-situ clusters. In contrast, in the right panel, we see an interesting correlation between eccentricity, distance at the pericenter, and GC type. Clusters with orbits of lower eccentricity have significantly larger distances at the pericenter than clusters with higher eccentricities. Their orbits are more circular. It is also interesting that ex-situ clusters show a lack of close circular orbits and have distances at the pericenter shifted to greater distances than in-situ clusters. This is an indication that they arrived in the MW along with dwarf galaxies.

In conclusion, there seems to be no strong observational data indicating the dependence of the N_2/N_{tot} - cluster mass correlation on the type of environment where GCs formed. This tells us, in our opinion, that the strength of tidal interactions of the just-forming galaxy is crucial in building the above correlation. In dwarf galaxies, GCs are formed closer to the center than in MW-type galaxies. As Figure 10 shows, the maximum mass of GCs does not seem to depend on whether they formed in-situ or ex-situ. This may suggest that the formation process of GCs is universal and depends on the strength of the tidal field and on the availability of gas. Ex-situ GCs have lower metallicity and are distributed in wider orbits with greater distance at the pericenter than in-situ GCs. Also, the ex-situ population lacks orbits with low eccentricity which may be related to events of close MW interactions with dwarf galaxies.

Figure 13 shows the comparison between observational data for MWGCs for all cluster populations and part of the population restricted to the in-situ GCs and with galactocentric distances smaller than 7 kpc and simulation results presented in this paper. Given that the choice of initial model parameters was not to reproduce the population of MWGCs but to determine the influence of individual model parameters on the evolution of observational cluster parameters, the agreement of simulation results with observations is satisfactory. In particular, the parameters of MWGCs in-situ and located relatively close to the MW center are reproduced satisfactorily in the simulations. Of course, as it was mentioned earlier R_h for models is a bit too large, and models with masses close to $10^6 M_\odot$ are missing. Using the results

presented in Section 3, it will be possible to select the initial parameters of the models to best match the observational parameters of the MWGCs.

In summary, to compare MOCCA simulations with observational data we should mainly focus on in-situ GCs with the radii of circular orbits below about 7 - 10 kpc. As was already mentioned in Section 2, the MOCCA code explicitly assumes a tidal field of the present MW. Taking into account the tidal fields of other types of galaxies, especially at the early stage of the evolution of GCs, would require the introduction of additional model parameters that are difficult to motivate physically.

4.2. MSP formation scenarios

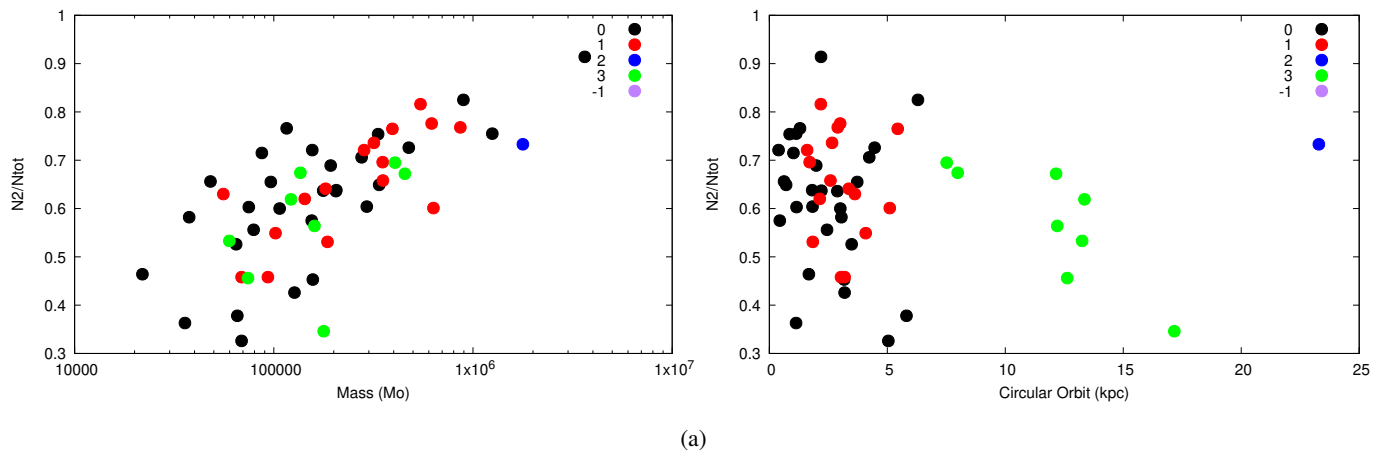
There are several scenarios in the literature for the formation of MSPs. In this Section, we will briefly discuss the scenarios and point out their weaknesses. We know from the literature on the topic that none of the proposed scenarios fully explain the process of MSP formation (e.g. Bastian & Lardo 2018). The most popular scenarios are:

1. AGB (e.g. D'Ercole et al. 2008; Bekki 2017; Calura et al. 2019)
2. Fast-Rotating Massive Stars and Interacting Binaries (e.g. Decressin et al. 2007)
3. The Early Disc Accretion Scenario (e.g. Bastian et al. 2013)
4. Very Massive Stars Due to Runaway Collisions (Gieles et al. 2018)

4.2.1. AGB Scenario

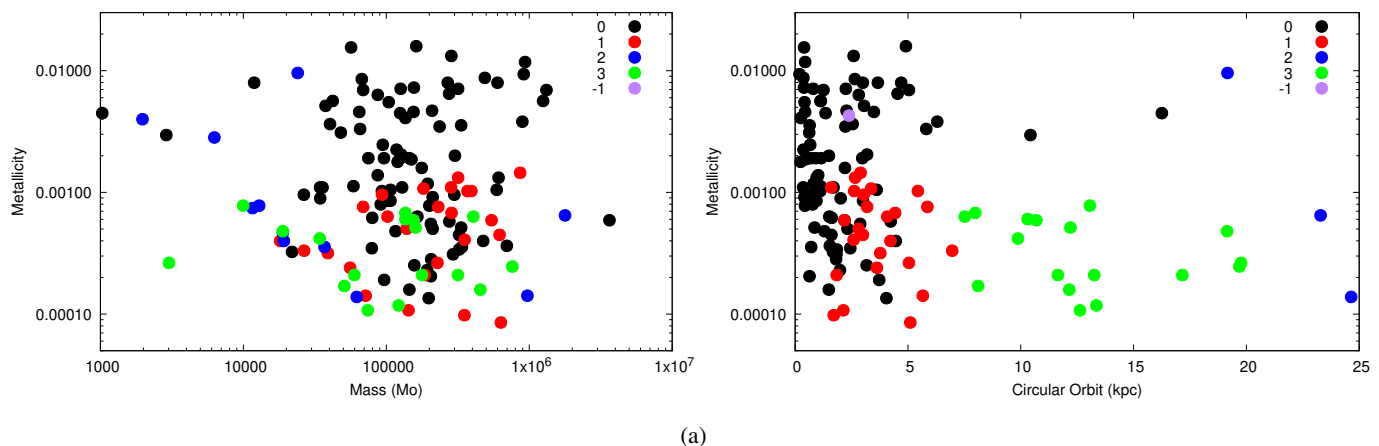
The AGB scenario has already been briefly discussed in the previous sections. It has been shown that the proposed TD-MSP scenario can explain the observed parameters of MWGCs providing a more open view of the initial conditions and the environment in which GCs live. This is about the migration of GCs, and the initial model not being in virial equilibrium. Therefore, we will now focus mainly on discussing the weaknesses of this scenario. It is important to note that there is no mass budget problem in this scenario. It is solved by assuming that POP2 is more centrally concentrated and the cluster is TF or close to TF and will lose a significant fraction of POP1 stars (e.g. Vesperini et al. 2021; Hypki et al. 2022, 2024).

In our opinion, the biggest weakness is the POP2 star formation process in a relatively dense gas and stellar environment. The question is, what physical conditions must be met for POP2 stars to form effectively in the dense environment of relatively massive and bright, heavily mass-losing POP1 stars? What is the efficiency of this process? Some of those questions were addressed a relatively long time ago by Conroy & Spergel (2011). They pointed out the importance of ram pressure, and accretion from the ambient interstellar medium on the development of young GCs and Type II Supernovae and prompt Type Ia Supernovae. They also provided some constraints on the initial properties of GCs and the early galactic environment. Unfortunately, their work was not followed by appropriate numerical simulations. The MOCCA models assume 100% efficiency, which is an unrealistic assumption. If star formation efficiency (SFE) is comparable to that of POP1, this means the mass of re-accreted gas becomes comparable to that of POP1. That is, we are back to the mass budget problem. It seems that models with a very small N_2/N_1 ratio may be the solution to this problem. In these models, a slow increase in the N_2/N_{tot} ratio is observed first, which then accelerates significantly after 1-2 Gyr and brings the ratio to the



(a)

Fig. 10. Left panel - dependence of the N_2/N_{tot} ratio on the present-day mass of MWGCs. Right panel - N_2/N_{tot} ratio vs the radius of the circular orbit. Dot colors indicate GC type, whether it formed in the MW or arrived with a dwarf galaxy absorbed by the MW: 0, black - in-situ formation, 1, red - ex-situ Gaia-Sausage/Enceladus formation, 2, blue - ex-situ Sagittarius dwarf, 3, green - ex-situ other mergers with dwarf galaxies, -1, purple - type not specified. Data are from catalogs: Milone et al. (2017); Bajkova & Bobylev (2021); Chen & Gnedin (2024); Baumgardt et al. (2019).



(a)

Fig. 11. Left panel - cluster metallicity (Z) vs present-day MWGC mass. Right panel - dependence of the cluster metallicity on the size of the circular orbit. A description of the color bar is given in the caption of Figure 10.

observed values, which is consistent with the absence of POP2 in clusters younger than 2 Gyr (e.g. Mucciarelli et al. 2007; Saracino et al. 2020). Initially, N_2/N_{tot} is of the order of 20-30% to be at the level of 5-7% after the formation of POP2 with SFE of about 30% and removal of the residual gas.

4.2.2. Fast-Rotating Massive Stars and Interacting Binaries

In this scenario, massive fast-rotating stars burning hydrogen in their interior transport, due to rotationally induced mixing, enriched material to the surface, which is later lost due to stellar winds and mixed with pristine gas left over from POP1 formation. Thus, POP2 formation occurs when the cluster is very young and its age is at most a few Myr. The problem of star formation efficiency discussed in the AGB scenario is even more relevant in this case. Let's remember that in such a young cluster, massive POP1 stars generate very strong radiation, which can significantly affect POP2 SFE. In addition, this problem is accentuated by the fact that in this scenario the POP1 formation occurs in a very dense nTF cluster. We know from simulations of the evolution of clusters consisting of a single population that in order to obtain compliance of the parameters of the simulated

cluster with the observational parameters, we must choose initial parameters that favor strongly nTF clusters (e.g. Askar et al. 2017). This means that even after ejecting residual gas left after the formation of POP1 and POP2, the cluster will still be nTF. From the work of Hypki et al. (2022, 2024), we know that for cluster models with MSP, if the cluster is nTF, the initial N_2/N_{tot} ratio remains virtually unchanged during cluster evolution. This means that virtually all remaining gas after POP1 formation would have to be used to form POP2 (assuming standard SFE=0.3). Additionally, in very dense clusters, the segregation time of the most massive stars is of the order of 1-2 Myr (e.g. Arca Sedda et al. 2024). This means that the mixing process of residual gas, after the formation of POP1, with the stellar wind of massive stars will mainly occur in the center of the cluster. This means that POP2 stars will mainly be created there. Thus, how to explain the observational fact (e.g. Bastian & Lardo 2018) also confirmed in MOCCA simulations by Hypki et al. (2024) that the N_2/N_{tot} ratio varies little depending on the distance from the cluster center? It is practically constant for distances R_h or greater. Also, how to explain very small variations of heavy elements between POP1 and POP2. To sum up, it seems that this

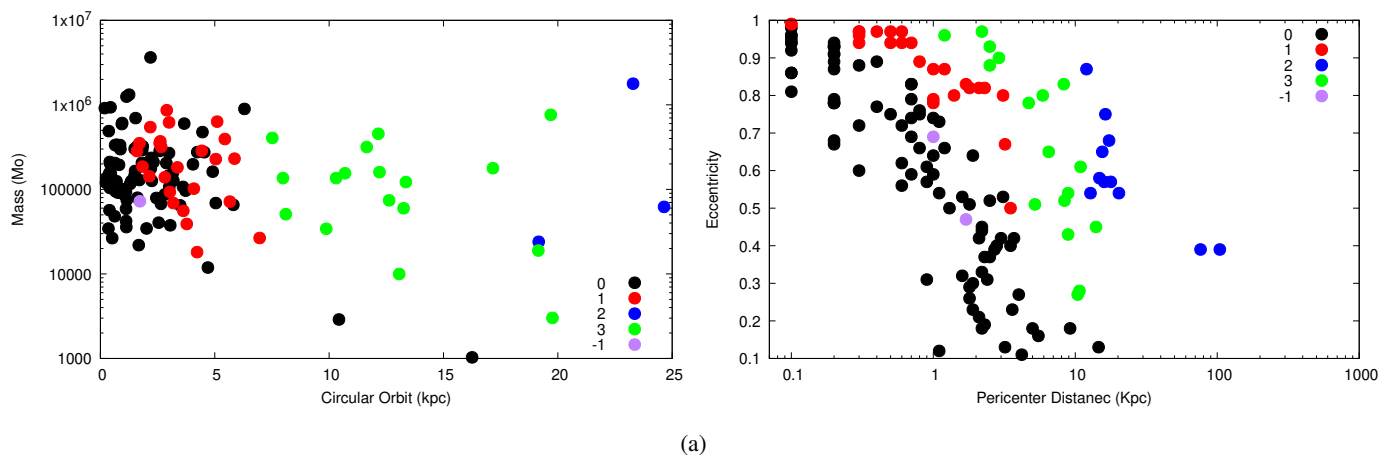


Fig. 12. Left panel - dependence of the cluster mass on the radius of the circular orbit. Right panel - dependence of the cluster orbital eccentricity on the orbit pericenter distance. A description of the color bar is given in the caption of Figure 10.

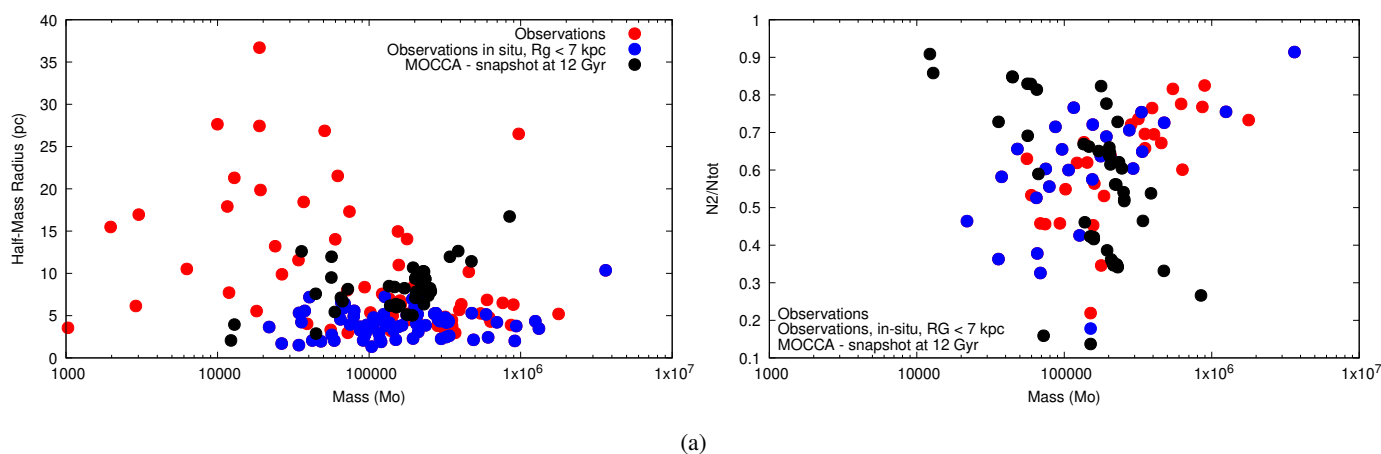


Fig. 13. Comparison between observational parameters of MWGCs and simulation results. Red dots observations, blue dots observations limited only to in-situ MWGCs and R_g smaller than 7 kpc, black dots simulations. Left panel – relation between cluster mass and R_h . Right panel – relation between cluster mass and N_2/N_{tot} ratio. Please note that the anti-correlation relationship between cluster mass and N_2/N_{tot} ratio observed in MOCCA models is purely artificial and is related to the choice of initial models. The nTF models and those initially located at large galactocentric distances cannot reproduce the observed parameters of MWGCs.

scenario has serious problems with a consistent explanation of the observed MWGC parameters.

4.2.3. The early disc accretion scenario

In this model, the enriched material ejecta from high-mass stars as well as from the fast-rotating massive MS stars is used to pollute low-mass stars that formed at the same time as the high-mass stars. The low-mass stars may retain the protoplanetary discs around them for about 10 Myr, which would sweep up the enriched material as they pass through the cluster core. The enriched material that was swept up by the discs would then eventually be accreted onto the host star. Even if we assume that initially POP1 stars were formed in small sub-clumps from which a cluster was then formed, we still have a problem with the fact that the newly formed cluster had to be nTF to be strongly mass-segregated. Additionally, the assembly process of clusters is fast, so sub-clumps cannot be strongly polluted by massive stars, because they are not yet fully formed. So, all the question marks raised in the previous Sections 4.2.2 are also valid for this scenario.

4.2.4. Very massive stars due to runaway collisions

In a very dense star cluster, a runaway collision process can form a very massive MS star (VMS) which releases hot H-burning processes through its stellar wind into the intracluster environment. This processed material mixes with pristine gas and forms further generations of stars until the VMS will form intermediate-mass BH or dissolve because of instabilities. Because the VMS can be continuously rejuvenated through stellar collisions, the amount of processed material ejected by the star can be several times the maximum mass of the star. The expected age of VMS probably cannot be larger than about 3–4 Myr. We know from many simulations (e.g. Portegies Zwart et al. 2004; Giersz et al. 2015) that the runaway collision process needs extreme densities and this means a very massive and strongly nTF cluster. Thus, the objections raised in the previous Sections to the proposed scenarios for the formation of VMS star apply in this case too. Additionally, the VMS star is characterized by very strong winds and radiation. The question is whether stars can form efficiently under such conditions, or whether material processed and mixed with pristine gas will escape from the cluster. It is possible that borrowing from a model in which protostellar

disks swept over processed material could help to create POP2, which will not only be located at the center of the cluster but also distributed throughout its volume.

In the next Section, based on the results from Section 3, observational data, and the above critical look at the MSP formation scenarios, we will try to describe the speculative scenario anchored in the AGB scenario framework.

4.3. Speculations

Our speculative scenario on the formation and evolution of GCs with MSP will be based on the results of simulations performed with the *moCCA* code and observational data, mainly kinematic and photometric. The scenario is rooted in the AGB model and will not attempt to explain the details of the observed correlations and anti-correlations between chemical elements. This will require detailed research beyond the scope of this paper. The focus is on trying to understand the global properties of MWGCs, namely the observed R_h , M , and N_2/N_{tot} ranges.

The masses of MWGCs are contained in the range of roughly $10^4 - 10^6 M_\odot$, R_h in the range of about 1 to 10 pc (larger radii have mostly ex-situ GCs), and the N_2/N_{tot} ratio in the range of about 0.3 to 0.9. An exceptionally strong constraint on models of MSP formation in GCs is the strong correlation between the mass of the cluster and the N_2/N_{tot} ratio. Simulations provide us with the following suggestions (when we talk about observational parameters, they are always compared with simulations in which the age of the cluster is 12 Gyr):

1. GCs just after the expulsion of the gas left over from POP1 formation should be TF or only slightly nTF. This means that they should form close to the galactic center. Too large galactocentric distances (keeping cluster mass constant) mean much larger R_t . It is difficult to imagine that a cluster with R_t of the order of several hundred parsecs would form as a TF cluster;
2. Only models in which the GC is TF or only slightly TF allow to achieve N_2/N_{tot} ratio within the limits observed for MWGCs;
3. Increasing the galactocentric distance for newly formed GCs with the same masses increases their R_h and decreases the N_2/N_{tot} ratio. This follows from the assumption that clusters are TF;
4. Models with smaller W_{01} guarantee larger values of the N_2/N_{tot} ratio. The larger the W_{01} the greater the mass, R_h and smaller the N_2/N_{tot} ratio;
5. The further a cluster is from virial equilibrium, the greater the N_2/N_{tot} ratio. The larger the Q_1 the smaller the mass, R_h and the larger N_2/N_{tot} ratio;
6. Migration of the cluster to larger galactocentric distances leads to an increase in cluster mass and R_h . The N_2/N_{tot} ratio remains virtually constant after migration.

The reaction of the observational parameters to the changes in global and environmental parameters discussed in the above points is summarized in Table 2.

Our goal is to determine the initial parameters of the models, including those related to the environment in which the clusters live, so that the observational parameters of the simulated clusters after 12 Gyr of evolution are within observational ranges. In our analysis, we focus only on in-situ GCs for which the apparent circular orbits are less than about 7 kpc.

GCs are formed in the very early stages of the galaxy's evolution, when the galaxy is a very hostile environment, with a

Table 2. The Table shows the reaction of observational parameters (M , R_h and N_2/N_{tot}) on changes the most important global and environment parameters: R_g , W_{01} , Q_1 and migration. \uparrow means increase, \downarrow means decrease, and $=$ means unchanged.

Parameter	M	R_h	N_2/N_{tot}
R_g	$=$	\uparrow	\downarrow
$W_{01} \uparrow$	\uparrow	\uparrow	\downarrow
$Q_1 \uparrow$	\downarrow	\downarrow	\uparrow
migration \uparrow	\uparrow	\uparrow	$=$

highly changing tidal field and multiple close and strong interactions with nearby dwarf galaxies. The mass of the galaxy is rapidly being built up during this period. The work of [Meng & Gnedin \(2022\)](#) suggests that the period of rapid changes in the tidal field of a galaxy ends after about 1 Gyr. After this time, GCs virtually stop migrating outside.

As many numerical simulations ([Banerjee & Kroupa 2013](#); [Leveque et al. 2022](#), e.g.) have shown, gas expulsion after the formation of POP1 is associated with strong cluster expansion and excess of kinetic energy relative to potential energy ($Q > 0.5$). Such a cluster will not exhibit a very high-density contrast (rather small W_{01} , significantly less than 5 or 6), and for small galactocentric distances it should be TF. The gas expulsion effect is mainly related to SFE and not to the position of the cluster in the galaxy. Thus, clusters that arise closer to the center have smaller R_t than those that arise further away, and can also more easily become TF or even TF overflowing.

The joint action of cluster migration and initial models with $Q > 0.5$ seems to work in the desired direction (R_h of a few pc and significant values of N_2/N_{tot}), provided that the massive cluster is formed relatively close to the galactic center (about 2-3 kpc), or the massive cluster experience stronger tidal field following its formation ([Meng & Gnedin 2022](#)). In order to obtain a model with a suitable range of observational parameters after a period of 12 Gyr of evolution, we should start with a TF cluster close to the center of the galaxy with a mass of at least $10^6 M_\odot$ and a bit out of virial equilibrium. Unfortunately, the above initial conditions do not guarantee the observed correlation between GC mass and N_2/N_{tot} ratio. To try to reproduce such a correlation, one should assume that the availability of gas from which GCs can form decreases with distance from the galactic center. Thus, clusters forming farther from the center will have, on average, a lower mass of POP1 and, more importantly, probably a significantly lower mass of gas that can again be accreted into the cluster and form POP2. As we know from the Section 3, the small value of N_2 relative to N_1 causes the increase in the N_2/N_{tot} ratio to be slow initially and only increase significantly after a period of 1 - 2 Gyr. Thus, if the cluster migrates during this time, its observed value of the N_2/N_{tot} ratio will be relatively low. For massive clusters formed from very massive gas clouds formed close to the galactic center, the availability of gas is very high, which will lead to the formation of clusters that initially have a relatively large N_2/N_{tot} ratio. For such clusters, the increase in this ratio to large values occurs quickly and then stabilizes. This means that their migration can stop the N_2/N_{tot} ratio at relatively large values. Dynamical friction also seems to be an important player in this process. We know that its effectiveness depends on the mass of the cluster and the distance from the center of the galaxy. Therefore, very massive clusters formed too close to the center or located after migration in not very eccentric orbits will be quickly "absorbed" by the nuclear star cluster. Those that have greater eccentricities

and large semi-major axes will survive (as can be observed for certain MWGCs). Less massive clusters are likely to migrate to larger distances and therefore dynamical friction will not be effective for them. Therefore, the mutual interaction of dynamical friction, migration, and availability of gas from which GC can be formed may lead to the generation of the currently observed correlation between the mass of GCs and their N_2/N_{tot} ratio.

This is a rather speculative and perhaps a bit naive scenario requiring several physical processes to operate in the right time order and in the right environment of the galaxy that is just forming and assembling. Maybe this is the answer to the question of why, for young and massive star clusters that we are now observing, we do not see the observational signatures of MSP. Simply, the current galactic environment is not suitable for the physical processes that enable the creation of MSP.

Of course, the scenario presented above does not mean that it is the only scenario explaining the observed properties of MSP in MWGCs. In our opinion, this is the leading scenario, responsible for the most important features of MSP. However, this is not the only scenario that may lead to the creation of MSP signatures. The scenarios discussed in the previous section may work simultaneously with the AGB scenario and lead to greater blurring of photometric and spectroscopic parameters of both POP1 and POP2. We would be surprised if the scenarios discussed above did not contribute to what is currently observed in MWGCs.

Finally, we should point out that according to the work [Ishchenko et al. \(2024\)](#) orbits of MWGCs undergo strong changes over Hubble time leading to their outwards or inwards migrations, which blur their initial parameters and introduce large scatter with their kinematic observational parameters.

5. Conclusions

In this work, we extended the model of the evolution of GCs with MSP presented in previous works [Hypki et al. \(2022, 2024\)](#). The model is anchored in AGB scenarios (e.g. [D’Ercole et al. 2008](#); [Conroy & Spergel 2011](#); [Bekki 2017](#); [Calura et al. 2019](#)). The possibility of delayed in time POP2 formation has been added. Technically, in the *moCCA* code, the POP2 formation process is defined by a number of parameters describing the properties of POP1, gas re-accretion, and POP2. The most important parameters are related to the migration of GCs in the galaxy, the mass of re-accreted gas, and the kinematic structure of POP1 (W_{01} , Q_1). All parameters are summarized in Table 1.

Based on more than 100 simulations, we analyzed the influence of the most important parameters on the evolution of the cluster and its observational properties after 12 Gyr of evolution. The aim of the study was to determine such parameter ranges so that the cluster model after 12 Gyr of evolution would best match the observational parameters of the MWGCs, in particular the cluster mass, R_h and N_2/N_{tot} ratio. In addition, observational data collected from the following MWGCs catalogs were analyzed: [Milone et al. \(2017\)](#) for N_2/N_{tot} ratios, [Bajkova & Bobylev \(2021\)](#) for kinematic parameters, [Chen & Gnedin \(2024\)](#) for origin types, and [Baumgardt et al. \(2019\)](#) for global parameters. Based on this analysis and the results of numerical simulations, a speculative scenario for the formation and evolution of GCs with MSP is presented. The results of the work can be summarized as follows:

1. The GC of POP1 should form near the center of its host galaxy and be very massive, so after removing the residual POP1 gas, it should be TF or close to TF. Close proximity to the galactic center means smaller R_l and much easier filling

of the Roche lobe after the ejection of residual gas. Only GCs that are initially TF can significantly increase the N_2/N_{tot} ratio during evolution. Large or very large initial mass means that after 12 Gyr of evolution, their mass still be considerable, at most as large as about $10^6 M_\odot$;

2. The time delay of gas re-accretion in the cluster relative to POP1 formation time causes the cluster to become nTF. According to the virial theorem, the addition of mass to the system is associated with a significant decrease in R_h . This causes a significant slowdown in the growth of the N_2/N_{tot} ratio during evolution;
3. Migration of GCs to larger galactocentric distances during the early time of galaxy formation causes a significant increase in R_l and thus the GC becomes nTF. Thus, the N_2/N_{tot} ratio practically stagnates;
4. The ejection of gas after the formation of POP1 is associated with a strong loss of cluster mass and potential energy. Thus, POP1 becomes too hot and $Q > 0.5$. It takes several tens of Myr to regain virial equilibrium, leading to a situation of increased loss of POP1 stars due to the cluster’s mass loss caused by the evolution of stars. The result of these processes is a very rapid increase in the N_2/N_{tot} ratio and a decrease in the mass of the cluster and R_h . This is a process that makes it possible, despite the effects of migration and gas re-accretion, to obtain the cluster’s observational parameters within the range of those observed for MWGCs.
5. The higher the number of POP1 and POP2 stars, the slower the cluster evolution (longer half-relaxation time). For N_2/N_1 ratio below 10%, we observe interesting behavior of N_2/N_{tot} ratio evolution. In the initial period up to about 1-2 Gyr, it remains practically constant in order to increase rapidly later and reach the values observed in MWGCs. The properties of these models allow us to hopefully better understand why YMSCs do not exhibit MSP signatures.
6. In addition to the correlation between mass and N_2/N_{tot} , MWGCs exhibit interesting kinematic features that are related to their place of birth. In-situ GCs have, on average smaller galactocentric distances and, on average greater metallicity and much closer pericentral distances than ex-situ GCs. In order to compare simulation results with observational data, we should limit ourselves only to in-situ GC. Numerical models have so far failed to take into account physical processes related to the close interactions of MW with dwarf galaxies.
7. To obtain an observational correlation between cluster mass and the N_2/N_{tot} ratio, we must combine the influence of the environment in which the cluster evolves with its internal evolution and the effects related to the ejection of the residual gas after POP1 formation. Massive clusters that formed close to the galactic center initially have a high N_2/N_{tot} ratio in regions with a high gas content before migrating outward. After migration, the ratio will not change significantly. If the orbit is close to, a circular massive cluster due to dynamic friction, will quickly merge with the center of the galaxy. If the orbits are highly eccentric with large semi-major axes, the efficiency of dynamical friction decreases and they can survive. The clusters that form further from the center are located in areas with lower gas availability and are therefore less massive and initially have a small N_2/N_{tot} ratio. This, together with migration, leads to the creation of a lower N_2/N_{tot} ratio than in massive clusters formed closer to the center of the galaxy. This is a bit of a speculative scenario and still needs to be confirmed in numerical simulations and observations.

It is very important to emphasize that models of GCs with MSP based on the AGB scenario require completely different initial models than models of clusters with a single population, or with multiple populations but no gas re-accretion, to reproduce the observational parameters of MWGCs. Namely, the first population needs to be TF or close to TF, and the second (subsequent) population should be much more concentrated than POP1. The requirement that POP1 is TF also imposes strong constraints on galactocentric distance. It must be of the order of a small few kpc. For a model with a single population or no gas re-accretion, it is required that the initial model be very strongly concentrated and nTF. Galactocentric distance in these models is not as important as for AGB scenario. Work is currently underway to further expand the *moCCA* code to include the ability to take into account GC motion in the galaxy's real, time-varying potential. For this purpose, based on cooperation with Peter Berczik's team, the machinery described in the work [Ishchenko et al. \(2024\)](#) will be used for integrating GC orbits in a MW-type galaxy, a galaxy that is currently forming and building its mass. The time-varying GC orbit (semi-major axis and eccentricity) will be used to determine the effective tidal radius and mass loss of GC. It is hoped that this will track GC migration and its impact on the N_2/N_{tot} ratio and other observational GCs parameters.

Acknowledgments

GM, AH, AA, GW were supported by the Polish National Science Center (NCN) through the grant 2021/41/B/ST9/01191. EV acknowledges support from NSF grant AST-2009193. AA acknowledges support for this paper from project No. 2021/43/P/ST9/03167 co-funded by the Polish National Science Center (NCN) and the European Union Framework Programme for Research and Innovation Horizon 2020 under the Marie Skłodowska-Curie grant agreement No. 945339. For the purpose of Open Access, the authors have applied for a CC-BY public copyright license to any Author Accepted Manuscript (AAM) version arising from this submission.

Data Availability

Input and output data for the globular cluster simulations carried out in this paper will be shared on request to the corresponding author.

References

Arca-Sedda, M. & Capuzzo-Dolcetta, R. 2014, *ApJ*, 785, 51
 Arca Sedda, M., Kamlah, A. W. H., Spuzem, R., et al. 2024, *MNRAS*, 528, 5119
 Askar, A., Szkudlarek, M., Gondek-Rosińska, D., Giersz, M., & Bulik, T. 2017, *MNRAS*, 464, L36
 Bajkova, A. T. & Bobylev, V. V. 2021, *Research in Astronomy and Astrophysics*, 21, 173
 Baker, J. G., Boggs, W. D., Centrella, J., et al. 2008, *ApJ*, 682, L29
 Banerjee, S., Belczynski, K., Fryer, C. L., et al. 2020, *A&A*, 639, A41
 Banerjee, S. & Kroupa, P. 2013, *ApJ*, 764, 29
 Bastian, N., Lamers, H. J. G. L. M., de Mink, S. E., et al. 2013, *MNRAS*, 436, 2398
 Bastian, N. & Lardo, C. 2018, *ARA&A*, 56, 83
 Baumgardt, H., Hilker, M., Sollima, A., & Bellini, A. 2019, *MNRAS*, 482, 5138
 Bekki, K. 2017, *MNRAS*, 469, 2933
 Bekki, K. 2023, *MNRAS*, 518, 3274
 Belczynski, K., Heger, A., Gladysz, W., et al. 2016, *A&A*, 594, A97
 Belczynski, K., Kalogera, V., & Bulik, T. 2002, *ApJ*, 572, 407
 Belloni, D., Askar, A., Giersz, M., Kroupa, P., & Rocha-Pinto, H. J. 2017, *MNRAS*, 471, 2812

Belloni, D., Kroupa, P., Rocha-Pinto, H. J., & Giersz, M. 2018, *MNRAS*, 474, 3740
 Breen, P. G. 2018, *MNRAS*, 481, L110
 Cai, M. X., Gieles, M., Heggie, D. C., & Varri, A. L. 2016, *MNRAS*, 455, 596
 Calura, F., D'Ercole, A., Vesperini, E., Vanzella, E., & Sollima, A. 2019, *MNRAS*, 489, 3269
 Chen, Y. & Gnedin, O. Y. 2024, *The Open Journal of Astrophysics*, 7, 23
 Conroy, C. & Spergel, D. N. 2011, *ApJ*, 726, 36
 Cordoni, G., Milone, A. P., Mastrobuono-Battisti, A., et al. 2020, *ApJ*, 889, 18
 D'Antona, F., Caloi, V., Montalbán, J., Ventura, P., & Gratton, R. 2002, *A&A*, 395, 69
 D'Antona, F., Vesperini, E., D'Ercole, A., et al. 2016, *MNRAS*, 458, 2122
 De Lucia, G., Kruijssen, J. M. D., Trujillo-Gomez, S., Hirschmann, M., & Xie, L. 2024, *MNRAS*, 530, 2760
 de Mink, S. E., Pols, O. R., Langer, N., & Izzard, R. G. 2009, *A&A*, 507, L1
 Decressin, T., Charbonnel, C., & Meynet, G. 2007, *A&A*, 475, 859
 Denissenkov, P. A. & Hartwick, F. D. A. 2014, *MNRAS*, 437, L21
 D'Ercole, A., D'Antona, F., Carini, R., Vesperini, E., & Ventura, P. 2012, *MNRAS*, 423, 1521
 D'Ercole, A., D'Antona, F., Ventura, P., Vesperini, E., & McMillan, S. L. W. 2010, *MNRAS*, 407, 854
 D'Ercole, A., Vesperini, E., D'Antona, F., McMillan, S. L. W., & Recchi, S. 2008, *MNRAS*, 391, 825
 Dondoglio, E., Milone, A. P., Lagioia, E. P., et al. 2021, *ApJ*, 906, 76
 El-Badry, K., Bradford, J., Quataert, E., et al. 2018, *MNRAS*, 477, 1536
 Forbes, D. A., Read, J. I., Gieles, M., & Collins, M. L. M. 2018, *MNRAS*, 481, 5592
 Fregeau, J. M., Cheung, P., Portegies Zwart, S. F., & Rasio, F. A. 2004, *MNRAS*, 352, 1
 Fregeau, J. M. & Rasio, F. A. 2007, *ApJ*, 658, 1047
 Fréour, L., Zocchi, A., van de Ven, G., & Pancino, E. 2024, *A&A*, 684, A181
 Fryer, C. L., Belczynski, K., Wiktorowicz, G., et al. 2012, *ApJ*, 749, 91
 Fuller, J. & Ma, L. 2019, *ApJ*, 881, L1
 Gieles, M., Charbonnel, C., Krause, M. G. H., et al. 2018, *MNRAS*, 478, 2461
 Giersz, M. 1998, *MNRAS*, 298, 1239
 Giersz, M., Askar, A., Wang, L., et al. 2019, *MNRAS*, 487, 2412
 Giersz, M., Heggie, D. C., Hurley, J. R., & Hypki, A. 2013, *MNRAS*, 431, 2184
 Giersz, M., Leigh, N., Hypki, A., Lützgendorf, N., & Askar, A. 2015, *MNRAS*, 454, 3150
 Gratton, R., Bragaglia, A., Carretta, E., et al. 2019, *A&A Rev.*, 27, 8
 Higgins, E. R., Vink, J. S., Hirschi, R., Laird, A. M., & Sabhahit, G. N. 2023, *MNRAS*, 526, 534
 Hobbs, G., Lorimer, D. R., Lyne, A. G., & Kramer, M. 2005, *MNRAS*, 360, 974
 Hong, J., Patel, S., Vesperini, E., Webb, J. J., & Dalessandro, E. 2019, *MNRAS*, 483, 2592
 Hurley, J. R., Pols, O. R., & Tout, C. A. 2000, *MNRAS*, 315, 543
 Hurley, J. R., Tout, C. A., & Pols, O. R. 2002, *MNRAS*, 329, 897
 Hypki, A. & Giersz, M. 2013, *MNRAS*, 429, 1221
 Hypki, A., Giersz, M., Hong, J., et al. 2022, *MNRAS*, 517, 4768
 Hypki, A., Vesperini, E., Giersz, M., et al. 2024, *arXiv e-prints*, arXiv:2406.08059
 Ishchenko, M., Berczik, P., Panamarev, T., et al. 2024, *A&A*, 689, A178
 Kamann, S., Dalessandro, E., Bastian, N., et al. 2020a, *MNRAS*, 492, 966
 Kamann, S., Giesers, B., Bastian, N., et al. 2020b, *A&A*, 635, A65
 Kamlah, A. W. H., Leveque, A., Spuzem, R., et al. 2022, *MNRAS*, 511, 4060
 King, I. R. 1966, *AJ*, 71, 64
 Kruijssen, J. M. D. 2015, *MNRAS*, 454, 1658
 Lacchin, E., Mastrobuono-Battisti, A., Calura, F., et al. 2024, *A&A*, 681, A45
 Langer, G. E., Hoffman, R., & Sneden, C. 1993, *PASP*, 105, 301
 Lee, J.-W. 2015, *ApJS*, 219, 7
 Lee, J.-W. 2023, *ApJ*, 948, L16
 Leitinger, E., Baumgardt, H., Cabrera-Ziri, I., Hilker, M., & Pancino, E. 2023, *MNRAS*, 520, 1456
 Leveque, A., Giersz, M., Banerjee, S., et al. 2022, *MNRAS*, 514, 5739
 Libralato, M., Bellini, A., Piotto, G., et al. 2019, *ApJ*, 873, 109
 Libralato, M., Vesperini, E., Bellini, A., et al. 2023, *ApJ*, 944, 58
 Lucatello, S., Sollima, A., Gratton, R., et al. 2015, *A&A*, 584, A52
 Lucertini, F., Nardiello, D., & Piotto, G. 2021, *A&A*, 646, A125
 Marino, A. F., Milone, A. P., Sills, A., et al. 2019, *ApJ*, 887, 91
 Martocchia, S., Bastian, N., Usher, C., et al. 2017, *MNRAS*, 468, 3150
 Mastrobuono-Battisti, A. & Perets, H. B. 2021, *MNRAS*, 505, 2548
 McKenzie, M. & Bekki, K. 2021, *MNRAS*, 500, 4578
 Meng, X. & Gnedin, O. Y. 2022, *MNRAS*, 515, 1065
 Milone, A. P. & Marino, A. F. 2022, *Universe*, 8, 359
 Milone, A. P., Marino, A. F., Da Costa, G. S., et al. 2020, *MNRAS*, 491, 515
 Milone, A. P., Piotto, G., Renzini, A., et al. 2017, *MNRAS*, 464, 3636
 Morawski, J., Giersz, M., Askar, A., & Belczynski, K. 2018, *MNRAS*, 481, 2168
 Mucciarelli, A., Ferraro, F. R., Origlia, L., & Fusi Pecci, F. 2007, *AJ*, 133, 2053
 Nardiello, D., Piotto, G., Milone, A. P., et al. 2015, *MNRAS*, 451, 312

- Niederhofer, F., Bastian, N., Kozhurina-Platais, V., et al. 2017, *MNRAS*, 465, 4159
- Parmentier, G. 2024, *ApJ*, 964, 140
- Portegies Zwart, S. F., Baumgardt, H., Hut, P., Makino, J., & McMillan, S. L. W. 2004, *Nature*, 428, 724
- Prantzos, N. & Charbonnel, C. 2006, *A&A*, 458, 135
- Saracino, S., Kamann, S., Usher, C., et al. 2020, *MNRAS*, 498, 4472
- Sollima, A. 2021, *MNRAS*, 502, 1974
- Szigeti, L., Mészáros, S., Szabó, G. M., et al. 2021, *MNRAS*, 504, 1144
- Tanikawa, A., Yoshida, T., Kinugawa, T., Takahashi, K., & Umeda, H. 2020, *MNRAS*, 495, 4170
- Vanbeveren, D., Mennekens, N., & De Greve, J. P. 2012, *A&A*, 543, A4
- Vesperini, E., Hong, J., Giersz, M., & Hypki, A. 2021, *MNRAS*, 502, 4290
- Vink, J. S. 2018, *A&A*, 615, A119
- Winter, A. J. & Clarke, C. J. 2023, *MNRAS*, 521, 1646
- Yaghoobi, A., Calura, F., Rosdahl, J., & Hagi, H. 2022, *MNRAS*, 510, 4330